REDUCING POLYMER ADSORPTION DURING CHEMICAL ENHANCED OIL RECOVERY IN UZEN FIELD

by

LAILA MARATBEKKYZY

THESIS SUPERVISOR

PEYMAN POURAFSHARY

Thesis submitted to the School of Mining and Geosciences of Nazarbayev University in Partial Fulfillment of the Requirements for the Degree of
Master of Science in Petroleum/Mining Engineering

Nazarbayev University
APRIL, 2023

ACKNOWLEDGMENT

As I reflect on completing this thesis, I am filled with immense gratitude toward the individuals who have supported me throughout this journey.

First and foremost, I want to take this opportunity to express my sincere gratitude to my honored supervisor, Professor Peyman Pourafshary. His broad research knowledge and professional background have been a continual source of support for me throughout my academic career. Meetings with my supervisor were vital to maintaining my progress on schedule and high motivation. This research work would not have been possible without his valuable suggestions and continuous support

I appreciate my research team members and friends' priceless assistance during these laboratory experiments. Special thanks to the best advisor Mariam Shakeel for her endless support and for giving me so much of her time to help me finish this thesis.

I want to take this chance to also acknowledge the School of Mines and Geosciences and its faculty for supplying me with all of the necessary equipment and technical advice for this project.

Last and definitely not least, I would like to highlight my most profound appreciation to my family for their everlasting love and support during the study.

ORIGINALITY STATEMENT

I, Laila Maratbekkyzy, hereby declare that this submission is my own work and to the best of my knowledge it contains no materials previously published or written by another person, or substantial proportions of material that have been accepted for the award of any other degree or diploma at Nazarbayev University or any other educational institution, except where due acknowledgment is made in the thesis.

Any contribution made to the research by others, with whom I have worked at NU or elsewhere is explicitly acknowledged in the thesis.

I also declare that the intellectual content of this thesis is the product of my own work, except to the extent that assistance from others in the project's design and conception or in style, presentation, and linguistic expression is acknowledged.

Signed on 05.04.2023

_____

ABSTRACT

This research investigated the potential of nanomaterials and alkaline in diminishing polymer adsorption on terrigenous rock formations. Polymer injection has been examined as a tertiary recovery technique in the Uzen field, which has favorable reservoir characteristics for this technology implementation. Nonetheless, the occurrence of polymer adsorption can considerably limit the usefulness of the method, reducing the permeability of the layers and the viscosity of the injection fluid, and consequently decreasing the oil recovery. Therefore, polymer adhesion may be adjusted by modifying the system's chemical and physical properties using nanoparticles. In particular, silica nanoparticles are widely employed due to their large surface area and ability to connect with polymeric chains. In addition, alkali can improve the repelling forces between the polymer and minerals by making the rock surface more negative.

This research aimed to determine the influence of silica nanoparticles and lye on HPAM-based ASP3 polymer adsorption at the interface of Uzen rock. It was investigated by performing tests on static and dynamic adsorption.

The first step was to evaluate different concentrations of polymers and nanoparticles by zeta potential measurement in order to achieve stable chemical conditions. ASP3 (2500 ppm) – SiO2 (0.1 wt. %) and ASP3 (2500 ppm) – NaOH (0.03%) solutions were utilized for the static adsorption tests, showing a noticeable influence on adsorption reduction. It should be highlighted that alkali was less efficient in prolonged durations, such as 24 and 36 hours.

When silicon dioxide was applied for dynamic adsorption studies, the adsorption of ASP3 was decreased by around 18%. At the same time, alkali was ineffective in reducing the polymer's dynamic adsorption, leading to a 5% increase in adsorption. Polymer-nanoparticle flooding as an enhanced oil recovery technique was successful, achieving a total recovery factor of around 96%, where incremental recovery was 5% higher than only the polymer injection case. Ultimately, it is recommended that the project plan for the Uzen field can be improved in consideration of the findings of the study.

TABLE OF CONTENTS

LIST OF FIGURES

LIST OF TABLES

1. INTRODUCTION

In recent decades, oil production has become more efficient and significantly larger by applying enhanced oil recovery techniques. Particularly chemical enhanced oil recovery (CEOR) plays a significant role in obtaining a high oil recovery factor, which is the primary goal of the oil industry. Depending on both reservoir and fluid characteristics, a specific type of CEOR method is used, namely polymer, surfactant, alkaline flooding, and foam drive. Polymer flooding (PF) and foam drive impact sweep efficiency at the macroscopic scale, while surfactant and alkaline flooding influence displacement efficiency at the microscopic scale.

Combined methods are even more effective, especially alkali-surfactant-polymer (ASP), polymer-alkali (PA), and polymer-surfactant (PS) floodings. The synergy of several chemical floodings maximizes the recovery factor:

- polymers enhance control of mobility by enlarging the viscosity of fluid that is used for reservoir oil displacement, as well as by making less contrast in permeability via covering areas with high permeability;
- surface-active agents reduce interfacial tension (IFT) that occurs between water and oil; this decrease in capillary forces consequently leads to growth in capillary number, finally releasing trapped oil;
- alkaline also lowers IFT and reduces the adsorption of surfactants and polymers.

The application of pilot EOR projects in Kazakhstani oilfields began in the early 1960s. The predominant challenges of most fields were associated with high water cuts, permeability heterogeneity, paraffin content, or oil viscosity. With the aim of incrementing oil production, the polymer injection was performed in the Kalamkas field resulting in higher vertical sweep efficiency (EI). EI was improved by 24% and 49% in selected two injection wells through lessening mobility ratio and viscous fingering (Bealessio et al., 2021).

As for potential projects, the Uzen field plans the injection of polymer. There are several reasons for choosing PF as a suitable method for the Uzen field. Firstly, appropriate reservoir fluid and formation properties to polymer injection. Secondly, a large water cut production of about 90% for the last five years till 2021. Thirdly, a high mobility ratio of above three because of high permeable channels. Such challenges can be controlled by making greater displacing fluid viscosity (Imanbayev et al., 2022).

Nevertheless, there are negative factors in the use of PF that limits the fruitfulness of this method. One of them is the adsorption of polymers which includes the entrainment of

particles, the adhesion of polymers to the surface of the rock, and the trapping. There are several reasons for this phenomenon, such as poor polymer design, obstruction of polymer particles in the complex pore system due to size difference, insufficient consideration of the formation mineralogy impact on the rock surface, and fluid interaction. It is also essential to control the effect of reservoir temperature, pH, the influence of the concentration of polymer, the structure of the polymer, reservoir heterogeneity, and salinity (Mohammed et al., 2020) As an example, the increment in brine salinity leads to the growth in the adsorption of polymer (Cheraghian, 2017). Likewise, when the concentration of the polymer goes up, the adsorption becomes greater (Al-Hajri et al., 2018).

Since the adsorption separates some polymer particles from the solution, polymer viscosity is substantially declined when the adsorption level becomes greater. Therefore, it limits the scale of recovery and leads to higher project costs. Thus, in order to reduce the adsorption mechanism nanoparticles (NPs) can be applied (Kakati et al., 2022). NPs are ultra-small-sized materials that perform ecologically safe, as well as cheap (Sun et al., 2017). The study conducted by Goshtasp Cheraghian et al. (2014) presents that silica and clay NPs play an essential role in decreasing the adsorption of polymer onto the surface of the rock, either sandstone or carbonate.

1.1 Problem Definition

As a result of the extensive waterflooding process, the Uzen oil field is currently experiencing a significant level of water cut. Eventually, recovering oil from the Uzen reservoirs is challenging, though polymer flooding has been found to be a successful technique. Nevertheless, a limitation known as adsorption diminishes the efficiency of polymer flooding by lowering the amount of polymer that reaches the oil reservoir and forming a coating on the rock surface that limits permeability. Ultimately, the potential volume of oil displaced will decrease, leading to negative economic consequences.

Alkaline solutions and nanoparticles have been recommended as a treatment for this problem due to their capacity to change the surface characteristics of the substrate and minimize polymer adsorption. Therefore, in order to improve the polymer flooding process, this study will test how adding nanoparticles or alkali to polymer solutions influences the adsorption values on terrigenous rock surfaces. Moreover, due to the deficiency of studies on the impact of both NPs and alkaline on the adhesion of polymer molecules on terrigenous deposits, conducting complex experiments on this topic is relevant.

In this investigation, encoded HPAM-based polymer ASP3, silica nanoparticles, and sodium hydroxide alkali were tested to determine the adsorption performance on two types of rock: Berea sandstone and Uzen rock consisting of polymictic sandstones and siltstones. As both rocks are related to terrigenous sediment rocks, Berea sandstone was chosen for trial experiments in order to define stable and appropriate solutions for further tests. In addition, injectivity and dynamic adsorption tests were also firstly using Berea core to obtain assumed results and make comparisons with outcomes of experiments on the Uzen rock.

The Uzen field conditions were applied for all core flooding tests. Oil displacement experiments were carried out to evaluate the efficiency of the decreased adsorption case in enhancing the recovery factor.

1.2 Objectives of the Thesis

1.2.1 Main Objectives

To diminish the adsorption of the suggested HPAM-based ASP3 polymer using CEOR techniques, the following objectives should be fulfilled:

- Analyze influencing factors on the polymer adsorption phenomenon
- Select the optimal concentrations of polymer-nanoparticles, polymer-alkali combinations by testing the stability of solutions
- Perform static and dynamic adsorption tests on Berea and Uzen rocks applying polymer, polymer-alkali, and polymer-nanoparticles solutions to conduct a comparison
- Develop oil displacement experiments using polymer flooding with and without nanoparticles to evaluate their effects on the recovery factor.

1.3 Scope of Work

The thesis is divided into several major chapters to have a systematic approach to obtain the achievement of polymer adsorption reduction.

Chapter 2 focuses on polymer flooding as a specific example of an enhanced oil recovery technology that can be used to address the production issues at the Uzen field. Moreover, it studies adsorption, which is the primary limitation of polymer flooding, and investigates ways to overcome the limitation, such as using alkaline solutions and nanoparticles.

Chapter 3 provides detailed information on used materials, and applied prime devices. Furthermore, it includes the design of all conducted experiments, including stability tests,

static and dynamic adsorption studies, injectivity investigations, and the displacement experiments of the oil.

Chapter 4 discusses and analyses obtained outcomes of implemented experiments. In this section, the impact of various chemicals combinations was investigated and compared after adsorption tests to identify the most favorable solution for displacing oil.

Chapter 5 summarizes the results of conducted studies, and provides the suggestions how to perform more effective research.

2. LITERATURE REVIEW

2.1. Uzen Oilfield's Production History and Problem Description

The Uzen field is one of the fifteen largest oil fields in Kazakhstan with about 496 million tons of initial recoverable reserves (KazMunayGas, 2017). The field was discovered in 1961 on the Mangyshlak peninsula. The Uzen formation consists of numerous layers and faults, with 23 different horizons ranging from 360 m to 2200 m deep used for oil production. The length of the field is nearly 39 km and its breadth is about 9 km (KazMunayGas, 2007)..

The initial saturation of oil in the reservoir is between 63% to 70%. In the case of intrinsic characteristics of the formation rock, the porosity varies between 21% and 25%, while permeability is in the range of 0.2-1 D (Bedrikovetsky, 1997).

The reservoir's original pressure levels were in the range of about 2200 to 2600 psi, and the temperature was between 54°C to 69°C. The field contains light crude oil with 10-25% paraffin depending on the location. However, as the crystallization temperature of the paraffin is approximately 50°C - 60°C, it led to issues throughout the system of production (Sparke et al., 2005).

The oil extraction process dates back to 1967 when cold Caspian seawater was injected into the reservoir of the Uzen field. According to the study by Bealessio et al. (2021), the application of 3°C water caused numerous challenges. Firstly, the solidified paraffin due to the cooling impact of untreated water eventually led to the pore-clogging predominantly in the zones of injectors. Secondly, water production was increased because of the plugged areas that caused the limitation in pathways to producers. Moreover, the side effect of the applied secondary EOR was the formation of various deposits, including corrosive precipitations. They were produced by the contact of seawater salts and formation oil, consequently contaminating both surface and subsurface facilities (National Intelligence Council, 1982; Bealessio et al., 2021, Mullaev et al., 2016).

Subsequently, a more successful method - a hot water injection project was designed. Conducting hot waterflooding was planned to correct the negative consequences of poorly managed oil recovery methods. The studies showed that it enhances well injectivity, limits paraffin damage, decreases the buildup of corrosion in equipment, and eventually displaces unrecovered reserves after cold waterflooding (National Intelligence Council, 1982; Mullaev et al., 2016). Finally, the performance of hot water injection at temperatures 85-90°C resulted in 34-38% of the oil recovery factor and comparatively slow water production (Bedrikovetsky, 1997; Mullaev et al., 2016).

The highest point of oil production, which was 16.249 million tons, was achieved in 1975. However, between 1976 and 1983, there was a significant decline in oil production by 35.5%, and an increase in water cut from 24% to 53.4%. This was attributed to a reduction in the amount of hot water injection, where hot water made up only 13% of the total injection volume in 1976, 27.7% in 1978, and 31.2% in 1979.

During the period of 1991-1999, the development of the Uzen field became unstable which resulted in a significant rise in the quantity of injected water and subsequently, the largest increase in water cut during the entire development period (Mullaev et al., 2016).

Nowadays, the Uzen field is experiencing a high degree of water production about 90%, which is a common issue in mature oil fields that have been subject to waterflooding for an extended period (Imanbayev et al., 2022). Moreover, considering the low recovery factor of the Uzen field, it would be reasonable to explore implementing tertiary recovery techniques to increase oil recovery. One such technique is Chemical Enhanced Oil Recovery, which has been successfully used in numerous fields worldwide.

In particular, the most common optimal solution for high water cuts is polymer flooding (Mahran et al., 2018; Navaie et al., 2022). The viscosity of the injected water is increased by the polymer, which enhances the oil-to-water mobility ratio and helps to improve sweep efficiency by smoothing out the displacement front in reservoirs with varying permeability (Abidin et al., 2012; Janiga et al., 2017). According to the investigations of Thomas (2016), on average, the use of polymer injections results in an additional 10% oil recovery compared to the original amount of oil in place (OOIP).

Nevertheless, polymer injection has a limitation known as adsorption, which is the tendency of polymers to stick to the surfaces of the reservoir rock, thereby decreasing the efficacy of the injection (Kurniadi et al., 2022). The presence of adsorption leads to a reduction in the quantity of polymer that reaches the desired oil reservoir, and the polymer that gets adsorbed may create a coating on the surface of the rock, impeding the permeability of the rock and limiting the flow of oil (Mishra et al., 2014).

Nanoparticles and alkaline solutions can be used to modify the surface properties of substrates and reduce polymer adsorption. The addition of nanoparticles into the polymer solution can create a physical barrier that prevents the polymer molecules from making contact with the surface, as well as generate a repulsive electrostatic interaction that reduces adhesion (Al-Hajri et al., 2021). Alkaline solutions can also decrease polymer adsorption by increasing the surface charge of the layer. In an alkaline environment, the substrate can

become negatively charged, which repels negatively charged polymer molecules (Hincapie et al., 2022). This repulsion results in a reduction in the polymer's ability to adhere to the surface.

It is important to note that the effectiveness of these methods in reducing polymer adsorption can depend on various factors, including the type of polymer and substrate used, as well as the size and concentration of the nanoparticles and the pH of the alkaline solution (Ambaliya & Bera, 2023).

2.2. Adsorption Mechanisms

In Enhanced Oil Recovery, adsorption pertains to the attraction and adherence of certain constituents in the injected fluids to the surface of the rock present in the reservoir.

EOR involves the injection of fluids, such as gas, water, or chemicals, into the reservoir to stimulate and move oil toward the production wells. However, some of the injected components may adhere to the rock surface through the adsorption process, which reduces their effectiveness in facilitating the displacement of oil. This may consequently decrease the efficiency of EOR and result in lower oil recovery (Belhaj et al., 2020).

The adsorption can be determined as physical or chemical adsorption that is differed from interaction behavior and influencing forces.

Physical adsorption considers adsorbed molecules under natural physical attractive forces on the adsorbent surface that usually have no bound with that surface, while in chemical adsorption there are electrons sharing processes between the adsorbent and adsorbate due to the direct bound contact (Webb, 2003; Liu et al., 2013).

In this way, the properties of adsorption will be considered in order to clarify the definition of each type. The physical type of adsorption is commonly reversible, a weak process that includes such interactions: as electrostatic and Vander Walls. The rate of adsorption is high, also it involves multi-layer creation. In terms of temperature, physical adsorption is mostly reduced with the temperature increment. With regard to the pressure factor, adsorption can be controlled by a decrease in pressure (Alsofi et al., 2017; Vidali et al., 1991; Dash, 2012).

In contrast to the physical type of adsorption, the chemical type of adsorption is an irreversible, stable process that involves chemical interactions. Moreover, only one layer will be created. When the temperature goes up, chemical adsorption also increases to a certain value of temperature, subsequently, it goes down regularly. In the context of pressure, an adsorption rate typically goes down with pressure growth. In some instances, the adsorption

process starts as physical, then continues as chemical after a certain period (Sagir et al., 2020).

The illustration of both adsorption types is shown in Figure 1 which clearly demonstrates acting forces and mechanisms.

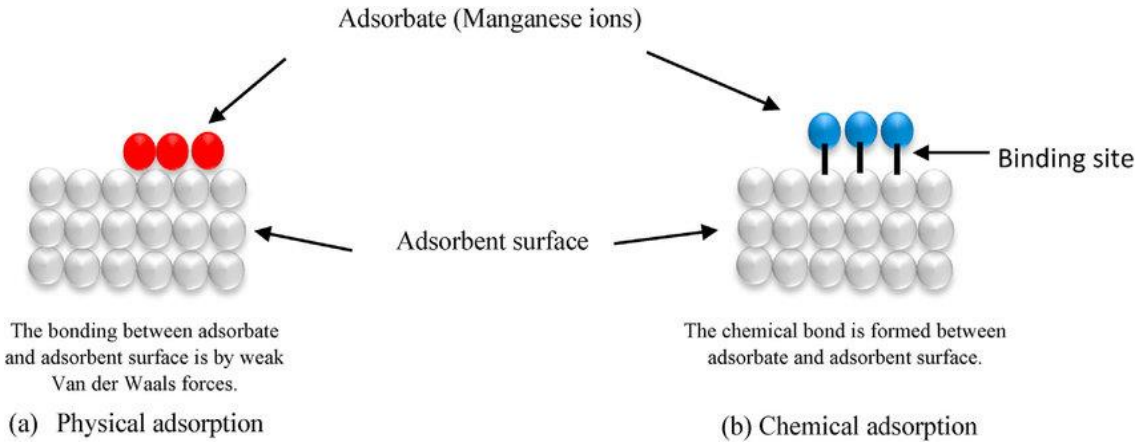

Figure 1. Types of adsorptions: (a) physical adsorption, (b) chemical adsorption and their interaction mechanisms (Rudi et al., 2020)

Several factors, including the characteristics of the injected fluids, reservoir rock composition, and the pressure and temperature conditions in the reservoir, influence the complex phenomenon of adsorption. Understanding and managing the adsorption process are crucial for optimizing the EOR process and achieving maximum oil recovery.

2.3. Adsorption of Polymers

Polymer molecules adhesion on the rock surface is a commonly irreversible process that causes a certain decrease in permeability and lowers initially aimed volumetric sweep efficiency (Zhu et al., 2021). Also, it is the single mechanism that extracts polymer out of the solution and leads to a substantial decrease in viscosity at large adsorption levels (Cheraghian et al., 2014).

2.3.1. Polymer Classification

The classification of polymers depends on their chemical structure and molecular weight (MW). CEOR processes frequently utilize polyacrylamides and biopolymers, which are two of the most commonly employed polymers (Firozjaii & Saghafi, 2020).

Synthetic polymers or polyacrylamides are produced by acrylamide monomer polymerization (Muhammed et al., 2020). The polymer has the form of powder or liquid emulsion. The average range of polyacrylamides (PAM) molecular weight varies around 0.2-30 million, where the value is determined by polymerization extent. As PAM is highly adsorbed on rock surfaces, they are partially hydrolyzed at the degrees of 15-35% in order to

decrease the adsorption (Zerpa, Colorado School of Mines). To recognize the difference in the chemical structure of mentioned synthetic polymers presented below Figure 2 is shown. So, therefore, partially hydrolyzed polyacrylamide (HPAM) is the most broadly applied polymer among synthetic polymers. It also has good stability characteristics related to temperature up to 160°C (Choi et al., 2014). In addition, HPAM has a relatively low cost, satisfactorily improves mobility ratio, excellent solubility in water, different forms of geometric structure that provide wider application, and high molecular weight – more than 10 million (Scott et al., 2020; Rellegadla et al., 2017). However, some disadvantages of HPAM are poor chemical and shear stabilities (Zerpa, Colorado School of Mines).

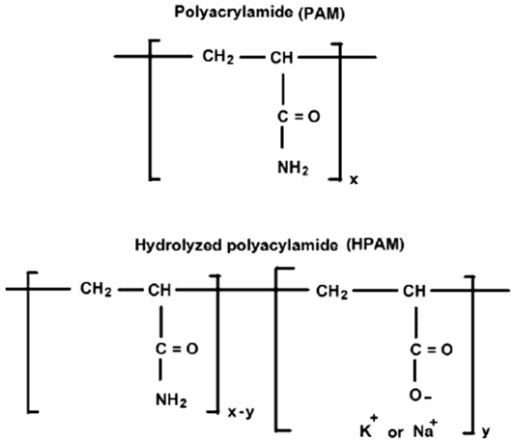

Figure 2. Chemical structure of PAM and HPAM (Gbadamosi et al., 2019)

Biopolymers or polysaccharides are generated by Xanthomonas campestris microbial action on the carbohydrate raw materials (Abbas et al., 2013). The variation of the average MW of biopolymers is nearly 1-15 million. The form of biopolymer may present as thickened broth or powder.

According to the investigations of Pu et al. (2018), xanthan gum (XG), guar gum (GG), and cellulose are good examples of biopolymers that can enhance the viscosity of injected fluids, leading to improved displacement efficiency and reduced fingering and channeling effects. The most popular type of polysaccharides is Xanthan gum which is typically stable for shear due to its branched chain, as well as at higher values of salinity (Sveistrup et al., 2016; Pu et al., 2018).

Additionally, these biopolymers can create gels within reservoirs, which can decrease permeability in highly permeable areas and redirect injected water to upswept regions. The gels may also lower water production in producer wells and increase oil recovery (Vossoughi & Putz, 1994).

Moreover, at low temperatures, biopolymers are capable of maintaining their viscosity, while in brines with high salinity and hardness, they exhibit increased solubility (Abbas et al., 2013).

Nevertheless, biopolymers have limitations such as a higher price, they are not stable at high temperatures, and low biological stability (Firozjaii & Saghafi, 2020). The structure of this biopolymer is illustrated in Figure 3.

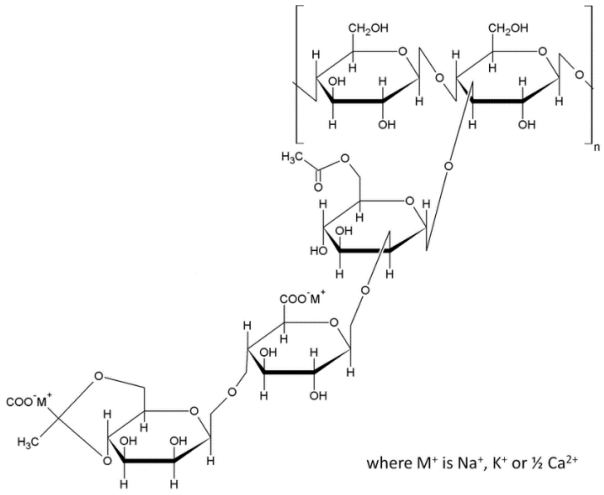

Figure 3. Xanthan gum chemical structure (Quinten et al., 2011)

2.3.2. Influence of Forces on Polymer Adsorption

Various forces affect the polymer adsorption process, including Van der Waals, electrostatic, and hydrogen bonding (Alsofi et al., 2017).

Van der Waals forces occur between two molecules due to fluctuations in electron density and become significant in polymer adsorption during the initial stages of contact between the polymer chains and the surface (Kotoulas et al., 2022).

When the surface and the polymer chains have different charges, electrostatic forces play a key role in polymer adsorption. The strength of these forces is dependent on the separation between the charged particles and the dielectric constant of the surrounding medium (Rellegadla et al., 2017).

Strong electrostatic attraction forces through hydrogen bonding between synthetic polymers and carbonate rocks lead to a large adsorption number of polyacrylamides. The same reason goes for the adsorption of negatively charged XG on limestone with a positive charge on the surface.

A chemical bond known as hydrogen bonding happens between molecules containing hydrogen atoms and electronegative atoms, such as oxygen, nitrogen, or fluorine. Hydrogen

bonding can play a significant role in polymer adsorption when the surface and polymer chains have hydrogen bonding sites (Zhang et al., 2019).

The mechanism of hydrogen bonding is demonstrated in Figure 4, which results in forming a layer of adsorption. When the polymers hold onto the surface of the mineral as a layer, there are some parts that cover the rock surface, whereas the rest segments are in contact with other chains because of hydrophobic interactions. Because of such interactions, when the concentration of polymers grows, the adsorption phenomenon will continuously gain higher values, so it presents as additional adsorption (Kamal et al., 2015).

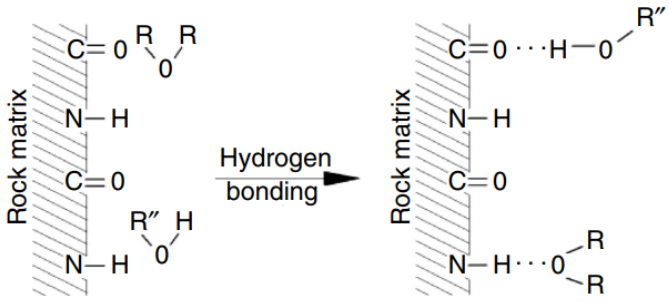

Figure 4. Hydrogen bonding mechanism (Zhong et al., 2015)

2.3.3. Influence of Mineralogy

The mineralogy of a rock surface has a significant influence on the adsorption of polymers onto that surface. In particular, the surface properties of minerals, such as their charge, area, and roughness, can impact the behavior of polymer adsorption.

The electrostatic interaction between a polymer and the surface of a mineral may be affected by the mineral's surface charge. Study by Al-Hajri et al. (2018) presented the impact of the rock surface on the adsorption level of several polymer types. Adsorption of the HPAM is higher on carbonate formations in comparison to the surface of silica as the polymer and carbonates are oppositely charged due to this having significantly attractive interactions. Actually, HPAM adsorption is much higher on kaolinite minerals than on Baker dolomite or calcium carbonate due to the structure and surface properties of kaolinite, as well as hydrogen bonding interactions (Rellegadla et al., 2017; Wang et al., 2017).

In the case of cationic polyacrylamide adsorption, the values are extremely larger on the surface of montmorillonite compared to quartzite.

The last considered polymer type was XG, the adsorption level was observed on the surfaces of kaolinite and siderite, consequently, it resulted in approximately very same retention value, respectively 16900 μg/g and 15600 μg/g (Al-Hajri et al., 2018).

If a mineral has a large surface area or is rough, there will be more places for polymers to stick to. Also, the specific minerals present can affect the behavior of polymers. The chemical characteristics of various minerals, such as polarity and hydrophobicity, can influence the way they interact with polymers. This implies that a mineral surface with greater hydrophobicity may have a greater attraction to a hydrophobic polymer (Ekanem et al., 2021; Lew et al., 2022).

2.3.4. Influence of the Concentration of Polymer

It is the main parameter in measuring the adsorption value of chemicals by providing a static test experiment. The difference between initial and final concentrations after conducting a static test for polymer shows the amount of adsorption.

When the concentration of polymer in a solution is low, it may not be sufficient to create a complete monolayer on the surface, which can result in an incomplete adsorption process and a limited amount of polymer being adsorbed (Park et al., 2015). Conversely, when the concentration of polymer is high, the molecules may start to bond with each other, creating clusters in the solution. These clusters may be too big to adsorb onto the surface or compete with individual polymer molecules for adsorption sites, thereby decreasing the total amount of polymer adsorbed (Mishra et al., 2014).

Zhong et al. (2017) made an investigation on the adsorption behavior of polymers at concentrations of 1000-2500 mg/L and concluded that there is an intensification in the adsorption mechanism with the increment in concentration.

How polymers get adsorbed is affected by various factors such as their chemical composition, molecular weight, and chain length. These factors play a significant role in determining the ability of polymer molecules to interact with other polymer molecules in a solution and the surface (Dang et al., 2014). It is important to note that the relationship between polymer concentration and adsorption is not straightforward and can differ depending on the system being studied. Sometimes, an ideal concentration range exists that maximizes adsorption, while in other cases, higher concentrations may result in reduced adsorption. For example, Al-Hajri et al. (2018) concluded that comparatively low and high concentrations of polymer indicate unnoticeable growth in adsorption than at medium amounts of polymer concentration.

2.3.5. Influence of Temperature

The adsorption of polymers can be significantly influenced by the temperature of the reservoir. Typically, when the temperature goes up, the solubility of the polymer in the

reservoir increases, causing a reduction in adsorption. This occurs due to the increased number of polymer molecules remaining in the solution, leaving fewer available to attach to the surface of the reservoir rock (Wiśniewska, 2011).

Nevertheless, the impact of temperature on polymer adsorption can be intricate and relies on multiple factors, including the type of polymer used, the composition of the reservoir fluid, and the characteristics of the reservoir rock surface. For instance, certain polymers may exhibit increased adsorption at elevated temperatures due to variations in the polymer chain's conformation or alterations in the surface properties of the reservoir rock (O'Shea et al., 2010).

Mohd et al. (2018) tested the impact of temperature on the viscosity of five various polymers, such as Polyvinylpyrrolidone, Arabic Gum, HPAM, XG, and Guar Gum. Results of the conducted test are demonstrated in Figure 5, where the temperature change is taken below 100°C. Accordingly, when the temperature becomes greater, there was a reduction in the viscosity of all five polymers. Nevertheless, the process of viscosity decreasing becomes more stable when the temperature exceeds 50°C for AG, PP, and HPAM.

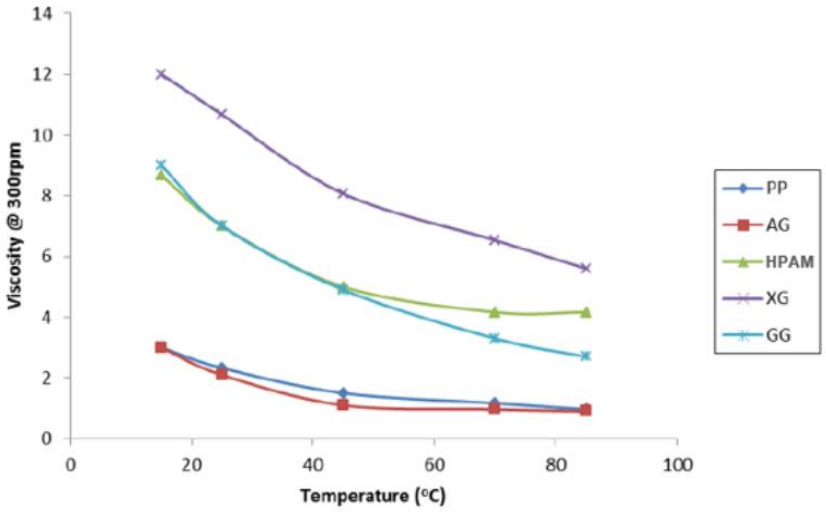

Figure 5. Effect of temperature on polymers viscosity (Mohd et al., 2018)

2.3.6. Influence of pH

The effect of the pH on adsorption varies depending on the type of polymer and the surface it is adsorbing onto. In accordance with the research of Wiśniewska et al. (2015), it can be concluded that at higher pH levels, there is a decrease in the adsorption of anionic PAM on the surface of alumina. It can be attributed to the presence of dissociated carboxyl groups in polyacrylamide molecules and the alteration in the charge of the alumina surface, which affects the adsorption behavior. Moreover, Kamal et al. (2015) reported that lower

adsorption degrees are obtained for anionic polymers on sandstone rocks if the pH has a value higher than 4.7 because of electrostatic repulsion.

In the case of limestone, when the pH level drops below 8.2, the carbonate becomes positively charged, resulting in a high adsorption rate of the anionic polymer. The adsorption of biopolymer XG is subject to the same principles (Kamal et al., 2015).

2.3.7. Influence of Salinity

Brine salinity is a key controlling factor that highly impacts the viscosity parameter of polymer. The majority of popular polymers that are usually synthetically typed have substantial sensitivity to high salinity reservoirs that leads to loss of polymer viscosity through the coagulation process. The rheological experiment of the researchers on the application of HPAM base polymers in carbonate reservoirs with high salinity pointed out that with the increment of salinity from 1000 ppm up to 4000 ppm of brine solution, the viscosity of those polymers went down due to the attraction force between cations of brine, more precisely Mg_2^+, Ca_2^+, Na^+ and negatively charged parts of polymer (Alfazazi et al., 2018).

Notwithstanding, it was mentioned that another type of polymer – biopolymers are not sensitive to salinity with great values. Quadri et al. (2015) study proved good toleration of biopolymer to 220 g/L or nearly 220250 ppm salinity. The reason for no change in polymer viscosity is the nature of the biopolymer which is non-ionic, as well as biopolymer molecule rigidness.

2.4. Reduction of Polymer Adsorption

Polymer flooding is a tertiary oil recovery technique that enhances the efficiency of oil extraction. The performance involves injecting a water-soluble polymer into the reservoir to enlarge the viscosity of the injected water and get a better mobility ratio between the injected fluid and the oil in the reservoir.

Nonetheless, a major challenge of PF is minimizing the polymer's adsorption onto the reservoir rock, which can decrease the success of the technique. This is because the adsorption can reduce the amount of polymer accessible to enhance the viscosity of the injected water and form a polymer gel that can obstruct the oil flow (Satken, 2021; Kamal et al., 2015; Park et al., 2015).

Decreasing the adsorption of polymer is significant for various reasons, such as enhancing oil recovery, minimizing expenses, and reducing the environmental effects of polymer flooding. The reduction of polymer adsorption leads to better performance of the

injected water to elevate the viscosity, which can facilitate the displacement of oil from the reservoir (Dang et al., 2011). Additionally, it requires a smaller amount of polymer to achieve the same viscosity enhancement, resulting in cost savings (Dang et al., 2014). Furthermore, decreasing the adsorption of polymer reduces the amount of polymer needed, which can mitigate the environmental impacts associated with the usage of a large amount of polymer that is not recovered (Ali & Barrufet, 1994). The application of nanoparticles and alkaline solutions can be an advantageous way to make less polymer adsorption by manipulating the physical and chemical properties of the system.

2.4.1. Application of Nanoparticles

As conventional and improved EOR methods face numerous challenges due to the complexity of formation characteristics, the application of nanotechnology is being viewed as a promising solution to address a significant portion of these issues. For instance, combining nanoparticles with polymers can lead to a decrease in water content, enhance macroscopic sweep efficiency, and result in a substantial increase in oil recovery. These outcomes are primarily due to the use of certain nanoparticles that decrease the adsorption of polymers (Udoh, 2021; Al-Hajri et al., 2021; Mohammed et al., 2020).

Nanoparticles are inexpensive material that has a size range of 1-100 nanometers, which is much smaller than the size of typical pores (Al-Hajri et al., 2021; Sun et al., 2017). This characteristic provides several advantages, such as easy flow and access to injection sites that are difficult to reach with traditional methods. Additionally, nanoparticles have a high surface-to-volume ratio, which means that there are more atoms on the surface of each nanoparticle, as clearly shown in Figure 6 (Sun et al., 2017).

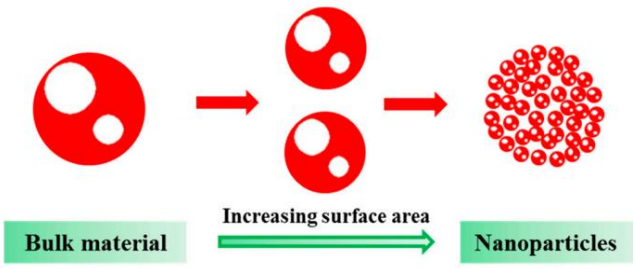

Figure 6. Surface-to-volume ratio increase of nanoparticles (Sun et al., 2017)

A mixture of NPs with base fluid generates a nanofluid that has several important mechanisms in EOR techniques. For instance, the nanofluid's NPs create a wedge-shaped film that is assembled by itself on the surface part of the oil phase due to structural disjoining pressure and contributes to the separation of droplets of oil from the surface of formation that

results in higher oil recovery (Wasan et al., 2011; Chengara et al., 2004). The structural disjoining pressure is intensified due to the higher particle density observed in nanoparticles with smaller sizes (Udoh, 2021).

The next form is a nanoemulsion which also has effective mechanisms, for example, it can efficiently improve mobility ratio, as well as shows good stability at high values of such factors as pressure, temperature, salinity, and shear (Zhang et al., 2018; Sun et al., 2017).

Moreover, NPs are an effective solution for the minimizing adsorption mechanism of polymer onto mineral surfaces. There are a number of mechanisms, such as steric stabilization, electrostatic adsorption, hydrophobic interaction, and competitive adsorption.

- Steric stabilization can be accomplished by nanoparticles that possess a substantial surface area, as they can act as a physical obstruction between the rock surface and the polymer. This obstruction inhibits the polymer from contacting the rock surface, ultimately diminishing its adsorption (Hall et al., 2010).
- Electrostatic repulsion between rock surface and polymer chains can occur if the nanoparticles carry a surface charge that is opposite to the charge on the polymer chains. For instance, if the nanoparticles have a negative charge, they will repel polymer chains with negative charges as well (Al-Hajri et al., 2021).
- Nanoparticles possessing a hydrophobic surface can generate a hydrophobic surrounding, obstructing polymer adsorption onto the rock surface. The reason behind this is that the polymer would rather remain in the aqueous solution than associate with the hydrophobic nanoparticles. This phenomenon is known as hydrophobic interaction (Xie et al., 2018).
- Due to their high surface area, nanoparticles can be adsorbed onto surfaces more easily than polymers, resulting in competitive adsorption. As a result, the polymer's adsorption onto the rock surface is reduced as there are fewer available adsorption sites (Bodratti et al., 2015).

There is a multiplicity of NPs that have been shown to reduce polymer adsorption onto rock surfaces in oil reservoirs, such as aluminum oxide (Al_2O_3), zirconium dioxide (ZrO_2), titanium dioxide (TiO_2), silica (SiO_2), magnesium oxide (MgO), and iron oxide (Fe_2O_3) NPs that are related to metal oxide NPs (Udoh, 2021). Other types are also applicable: a magnetic, organic, and inorganic NPs (Ruiz-Cañas et al., 2020).

The selection of certain types depends on multiple factors including the particle size and shape, surface charge, polymer concentration, ionic strength of the solution, pH, and temperature.

- The capacity of NPs to adsorb onto rock surfaces can be influenced by their size and shape, as smaller particles may infiltrate deeper into rock pores, and certain particle shapes may exhibit a greater attraction to particular rock surfaces (Ruiz-Cañas et al., 2020).
- The adsorption behavior of NPs can be affected by their surface charge, as positively charged particles are drawn to negatively charged rock surfaces while negatively charged particles are repelled (Corredor Rojas., 2019).
- Elevated levels of polymer concentrations can enhance the adsorption process, but there exists a saturation point beyond which additional increases in concentration do not have a significant impact. On the other hand, heightened ionic strength can diminish electrostatic interactions and lead to a decrease in adsorption (Al-Hajri et al., 2021).
- Changes in the pH level of the solution can influence the surface charge of both the nanoparticles and the rock surface, which can have an effect on adsorption (Corredor Rojas., 2019).
- The ability of nanoparticles to interact with the rock surface can be influenced by fluctuations in temperature, which can also impact their kinetic energy (Ruiz-Cañas et al., 2020).

Silica NPs are commonly used to reduce polymer adsorption on rock surfaces. These nanoparticles possess a large surface area and can be modified with surface functional groups that can interact with polymer molecules and prevent their attachment to the rock surface (Cheraghian et al., 2014). Also, SiO_2 application is suitable for sandstones that have a water-wet system, as well as carbonates that have an oil-wet system. In this case, important to take into consideration the permeability of the formation, as at low values of permeability the concentration of SiO_2 becomes a critical factor, so higher values of silica NPs concentrations tend to plug porous medium (Sun et al., 2017).

Al-Hajri et al. (2021) conducted research on the action of silica NPs with a weight percentage (wt. %) of 0.01-0.1 on lowering of HPAM (with different MW) adsorption on shale formation which is illustrated in Figure 7. Near to half a decrement in the value of polymer adsorption was obtained due to the reduction in the contact area between the polymer and shale surface. It is important to note that the higher the MW of HPAM the larger the adsorption value.

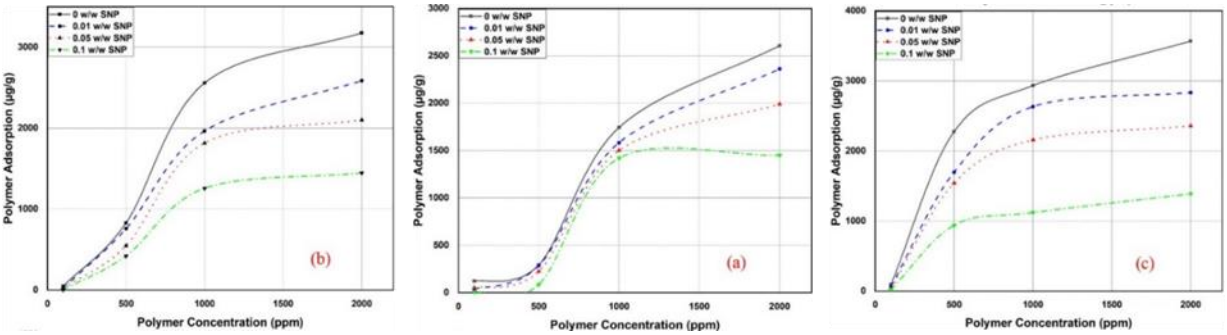

Figure 7. Reduction in adsorption at different HPAM concentrations: (a) low MW, (b) medium MW, and (c) high MW (Al-Hajri et al., 2021)

Another study of the effect of SiO_2 on the decrease in the adsorption of polymer molecules was carried out by Li et al. (2019). Figure 8 presents that the adsorption capacity of GG on sandstone initially increases rapidly, but eventually slows down in the period of 2-3 hours and reaches a stable state after 3 hours. Notwithstanding, adding 2000mg/L silica NPs causes a considerable shift in the curve, decreasing the mean rate of adsorption from 30.8 ug/min to 16.7 ug/min. Finally, the adsorption of the polymer went down by about twice.

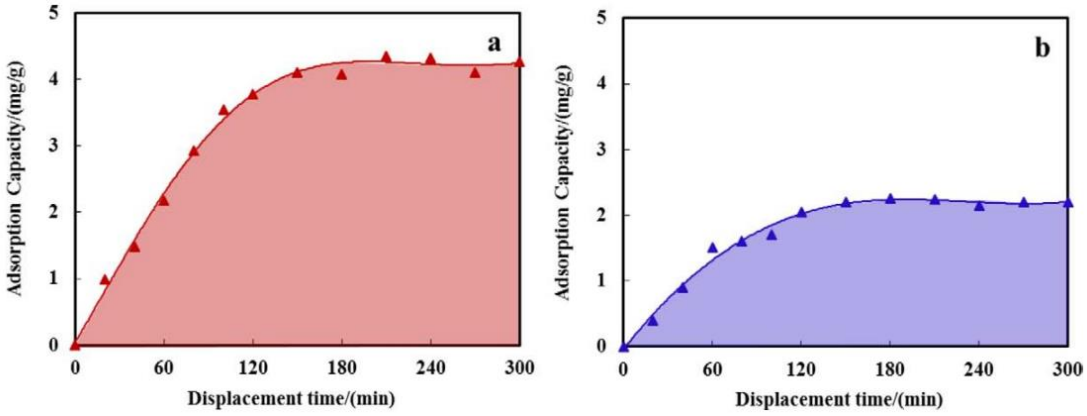

Figure 8. The capacity of Hydroxyl Guar Gum for adsorption changes over time: (a) without SiO2, (b) with SiO2 (Li et al., 2019)

2.4.2. Application of Alkali

Alkali is a potential chemical that could be utilized to lessen polymer adsorption on the rock. There are many types of alkaline, such as sodium hydroxide (NaOH), sodium carbonate (Na_2CO_3), sodium orthosilicate (Na_4O_4Si), ammonium carbonate [$(NH_4)2CO_3$], sodium metaborate ($NaBO_2$), ammonium hydroxide (NH_4OH) but popular ones are NaOH, Na_4O_4Si, and Na_2CO_3 (Sheng, 2013).

Alkali can be used in a variety of ways, including alkali solutions injection or the addition of alkali to the polymer solution, to change the characteristics of rocks. The type of alkali used, its concentration, the solution pH, and the composition of the rock have an

impact on the performance of alkali treatment. As the charged molecules of polymer and charged surfaces of rocks interact electrostatically inducing adsorption, alkali treatment can be used to change the mineral surface charges (Kazempour et al., 2012; Dang et al., 2011; Krumrine & Falcone., 1983). It may also alter the wettability of the rock surface, which could have an effect on how fluids flow within the reservoir. By improving the water-wetting of the rock's surface, it can enhance how injected water will displace oil (Ghalamizade Elyaderani & Jafari., 2020).

Based on the study of Nurmi et al. (2022) the presence of alkali reduces the adsorption of HPAM on the Berea sandstone. The outcome of the static adsorption test without additional sodium carbonate was 31 g/g. The result was considerably better for the alkali-added case that result in 24 g/g. Moreover, there was observed that the softening of brine has an impact on the adsorption phenomenon. Therefore, both experimental findings were substantially lower compared with the case that used a hard brine, where 48 g/g HPAM adsorption was obtained. It may be concluded that removing magnesium and calcium salts from the brine decreased adsorption and that raising the pH may have had an additional impact.

In addition, Dang et al. (2011) concluded that when alkaline is present, the adsorption of the polymer HPAM becomes significantly less. This is caused by the presence of two pH-sensitive functional groups in the polymer, with carboxyl groups playing a major role in regulating its rheological properties. When the pH is high, the carboxyl groups separate, creating strong repelling negative charges on the rock surface. As a result, polymer adsorption significantly declines. The carboxyl groups become negatively charged and reject the rock surface due to electrostatic forces when sodium carbonate is added.

On the other hand, certain cases that have negative or ineffective impacts on polymer flooding tests are also present. For instance, based on the findings of Sheng (2017), due to the higher salt content that the alkali causes, the addition of alkali might produce a reduction in the viscosity of polymers. Moreover, Ma & Pawlik (2005) conducted research on the influence of sodium carbonate on the adhesion of GG molecules on quartz. Consequently, the polymer that has a high MW was significantly adsorbed on the surface of quartz because of the metal cations presented in alkali. However, the adsorption of GG with low MW was not influenced by alkali cations.

Overall, alkali has a complex effect on polymer adsorption on rock surfaces and is controlled by a number of variables.

3. METHODOLOGY

This chapter describes a methodical strategy for investigating the effects of caustic soda and silica nanoparticles on polymer adsorption onto Uzen field rock. The selection of certain materials was based on their suitability for the conditions of the target field, particularly the stability of chemicals at 63°C reservoir temperature and in the formation and seawater brine concentrations of approximately 14000 ppm. The methodology includes multiple sections, including applied materials descriptions; main devices, and systems specifications; as well as, conducted procedures.

Firstly, stability tests were performed to screen for optimum combinations of NP-polymer and alkali-polymer at various concentrations using synthetic seawater (SSW). The concentration of the SSW was the same as seawater (RSW). After checking the visual stability of solutions, they were tested for zeta potential analysis through Zetasizer to confirm the stability characterizations. It should be noted that stability tests were repeated several times for the clarity of the experiments.

Secondly, obtained favorable mixtures were tested by static adsorption tests. To determine the effect of selected SiO_2 and NaOH on the ASP3 HPAM-based polymer adsorption, four different SSW-based solutions were prepared, and the adsorption on the crushed Berea sandstone was measured. Afterward, when acquired samples were analyzed by use of a UV-Vis Spectrophotometer, a static adsorption experiment was repeated with sustainable RSW-based solutions on crushed Uzen formation rock. The outcomes of the two static adsorption experiments were compared.

Third, a variety of core flooding tests including injection tests, dynamic adsorption experiments, as well as oil displacement tests were carried out to observe adsorption behaviors in reservoir conditions. As a sample for trial dynamic adsorption and injectivity tests, Berea sandstone was selected to get the expected values of adsorption, resistance factor (RF), residual resistance factor (RRF), and mechanical degradation.

All outcomes were interpreted and described in detail in the following sections.

3.1. Materials

Applied materials for all conducted experiments inclusive of chemicals, brines, oil, and samples of rocks were clearly described with appropriate illustrations.

3.1.1. Rock Samples

For all studies, two types of rocks were employed. For static adsorption tests, Berea and Uzen formation cores were crushed to be applied as samples. Regarding core flood experiments, one Berea sandstone core as Sample 1, and six Uzen field cores were utilized. In particular, Sample 2 was applied to the injectivity test, and Samples 3-5 used for dynamic adsorption tests: polymer, polymer/alkali (P-A), and polymer/nanoparticles (P-NP). The last two samples were utilized for oil displacement experiments, applying polymer and P-NP. The properties of all these samples are presented in Table 1. The illustration of the Uzen core is shown in Figure 9.

Table 1. Characteristics of core samples used for core floodings

Sample ID	L, cm	ID, cm	PV, cm^3	BV, cm^3	Ø, %	$\rho_{(rock)}$, g/cm^2
1	7.89	3.73	18	86.17	20.9	2.65
2	5.39	3.79	16	60.33	26.5	2.66
3	5.76	3.78	17.2	64.64	26.6	2.66
4	5.55	3.78	16.3	62.28	26.2	2.66
5	5.51	3.79	16.2	62.16	26.1	2.66
6	5.55	3.79	15.2	62.48	24.3	2.66
7	5.57	3.78	15.6	62.42	25.0	2.66

Figure 9. Saturated Uzen core sample

3.1.2. Brines

Generally, three types of brine were utilized during the adsorption testing. Synthetic seawater with a concentration of 14248.7 ppm was used for all types of tests along with

Berea rock. An ionic composition of SSW is shown in Table 2. A Caspian seawater sample at a concentration of 14300 ppm and hardness of 80-120 ppm was applied for both static adsorption and core flood experiments. A formation water having a concentration of about 51000 ppm and hardness of 254 ppm was used as a pre-flush for oil recovery tests to achieve the condition of the reservoir.

Table 2. Synthetic seawater composition by ions

Ions	Concentration, ppm
Na^+	3513.1
Ca^{2+}	400.8
Mg^{2+}	790.4
Cl^-	6026.6
$(SO_4)^{2-}$	3138
$(HCO_3)^-$	256.2
K+	87.6
$(CO_3)^{2-}$	36

3.1.3 Crude Oil

The Uzen field crude oil was used in this study. The viscosity of the crude oil at the reservoir temperature of 63°C was 8 cP. There are considerable amounts of asphaltenes about 13 wt. % and paraffin by 20 wt. % in the oil (Imanbayev et al., 2022). Also, the density of oil in reservoir conditions is 787 kg/m^3. The oil was filtered before core flooding.

3.1.4 Chemicals

In this project, three types of chemicals (polymer, nanoparticles, and alkali) are used for several purposes. To estimate the adsorption of ASP3 on the Uzen rock surface, silica nanoparticles and caustic soda were implemented. All three chemicals were applied to evaluate the efficiency to displace more oil through the porous media.

3.1.4.1. Polymer

Throughout this project, the white crystal-powdered HPAM-based polymer ASP 3 was employed which is presented in Figure 10. The polymer hydrolysis degree is 6.4%. The bulk density of the polymer is 600 kg/m^3, intrinsic viscosity is 12.9 dl/g, molecular weight is

7.6 g/mol, and the content of the main substance is 92.28%. Our previous studies showed that the ASP3 polymer is compatible with the field conditions (Yerniyazov et al., 2023).

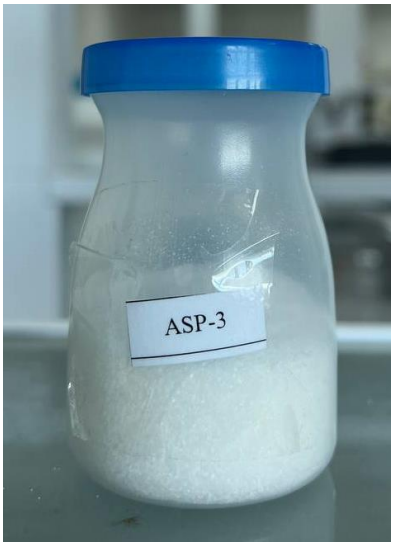

Figure 10. Encoded ASP3 polymer on basis of HPAM

3.1.4.2. Nanoparticles

Silicon Oxide Nanoparticles were chosen for the project following studies that indicated the considerable suitability of SiO_2 for enhancing the adsorption of HPAMs (Cheraghian et al., 2014). Negatively charged silica particles can be engineered to repel negatively charged HPAM molecules, preventing them from adhering to rock surfaces.

The material was provided by SkySpring Nanomaterials company. It is a spherical-shaped porous silicon oxide powder with a purity of 99.5%. The size of the material ranges from 10 to 20 nanometers with a density of 2.4 g/cm3.

3.1.4.3. Alkaline

As an alkaline sample, sodium hydroxide was selected due to its compatibility with the chosen polymer, high solubility, and strong base (Jung et al., 2013). The purity is more than 97% and is provided by SIGMA-ALDRICH.

The surface charges of rocks can be changed with NaOH to make the negatively charged HPAM molecules less attractive to them. Moreover, by destroying any bonds that may already exist between the HPAM molecules and the rock surface, the application of NaOH can also assist to reduce the adsorption of the HPAM molecules. The use of NaOH must be carefully regulated since it may react with other reservoir components and result in undesirable side effects.

3.2. Experimental Procedure

3.2.1. Preparation of SSW and Chemical Solutions

Depending on the type of experiment, several preparation techniques were used for chemical solutions including polymer, polymer-nanoparticles (P-NP), and polymer-alkaline (P-A).

3.2.1.1. Synthetic Seawater Solution

A specific volume of distilled water was added to the beaker based on the required solution volume. For instance, the necessary quantity of salts, which is stated in Table 3, was added to distilled water at 700 rpm of stirring and mixing to make the synthetic brine. To get a complete solution in the water, each salt was added at intervals of around 4-5 minutes. Then the beaker of brine was coated with parafilm and was left for 1-2 hours for mixing with cover.

Table 3. Synthetic seawater brine composition

Required salts	Chemical formula	Added mass, g/L	Producer companies
Sodium chloride	NaCl	4.797	SIGMA-ALDRICH
Potassium chloride	KCl	0.167	SIGMA-ALDRICH
Calcium chloride	$CaCl_2$	1.11	SIGMA-ALDRICH
Magnesium chloride hexahydrate	$MgCl_2*6H_2O$	6.611	SIGMA-ALDRICH
Sodium sulfate	Na_2SO_4	4.64	SIGMA-ALDRICH
Sodium carbonate	Na_2CO_3	0.064	SIGMA-ALDRICH
Sodium bicarbonate	$NaHCO_3$	0.353	SIGMA-ALDRICH

3.2.1.2. Polymer Solution

For stability tests, the polymer solution was prepared in three different concentrations based on our previous studies, as 1000 ppm, 1500 ppm, and 2500 ppm.

The SSW was first prepared, then after 30 minutes of stirring at 700 rpm, the polymer was added. Formula 1 was used to calculate the required weight of polymer powder for the solution:

$$W(p) = \frac{C(p) \times V(b)}{10^6} \quad (1)$$

where,

$W(p)$ – polymer weight, g

$C(p)$ – polymer concentration, ppm

$V(b)$ – brine solution volume, mL

For instance, to get 200 mL of polymer solution at the concentration of 1000 ppm, 0.2 g of ASP3 polymer was added, while 0.3 g for 1500 ppm, and 0.5 g to obtain 2500 ppm. The preparation of the polymer solution was in line with the API recommended practice 63 (API, 1990). Utilizing a magnetically driven stirrer, the bottom of the liquid vortex should reach 75% of the mixture. To avoid breakage of polymer chains due to high agitation speed, the mixture rate was immediately switched to 100-150 rpm, otherwise, it can result in a decrement in polymer viscosity. The mixture was mixed for 2 hours to achieve a completely dissolved solution.

For adsorption and core flooding tests using the Uzen core, seawater was utilized as a base for the polymer solution. Therefore, the measured polymer amount was directly added to the seawater for mixing. In this instance, the previously indicated steps by API were also followed.

3.2.1.3. Nanoparticle-Polymer Solution

Various types of P-NP solutions were prepared for several purposes, such as investigating the stability of mixtures at different concentrations of SiO_2, selecting the most stable solution at different polymer concentrations, and observing the performance of NPs in reducing the adsorption of ASP3. As an example, to make the P-NP solution in SSW, 200 ml of ultrapure distilled water was mixed with 0.2 g of SiO_2 to obtain 0.1 wt% of NP in the solution. A magnetic stirrer was then used to thoroughly mix the solution for 30 minutes at 600 rpm. The solution was then put into Ultrasonic Homogenizer for one hour at 70°C. The device parts are shown in Figures 11 and 12.

Figure 11. Intelligent ultrasonic processor

Afterward, before adding 0.2 g of ASP3, the solution was cool down to prevent the thermal degradation of the polymer. The polymer was added to the nanofluid and stirred at a lower speed (150 rpm) to avoid mechanical degradation of polymer molecules. After 30 min of mixing, the required mass of salts listed in Table 1 was added and mixed for 2 hours to ensure uniform dispersion. This procedure was repeated for other polymer concentrations (1500 ppm and 2500 ppm). Moreover, stability tests were also conducted with SiO_2 concentrations of 0.05 wt% and 0.3 wt%, where the polymer concentration was 2500 ppm.

Figure 12. Ultrasonic cell crusher noise isolating chamber

In the case of P-NP mixture preparation in the Caspian seawater, SiO_2 was directly mixed with the seawater. Other steps were the same as for the SSW case excepting salts addition.

3.2.1.4. Alkali-Polymer Solution

As the alkaline sample, 0.5 M of NaOH was used. Primarily, the alkaline solution with concentrations of 1% was prepared by adding 2g of alkaline to 200 mL of the ultrapure distilled water, then mixed for 20 min. The pH value of the solution was 13.04. Subsequently, 200 mL of SSW was prepared, then about 3-4 mL of 1% alkali were added to the brine. So, the NaOH concentration was in the range of 0.02-0.04%, which resulted in a solution with a pH value of 8.23-10.01. Finally, 0.2 g of Polymer with a concentration of 2500 ppm was added into the alkaline solution respecting API instructions and left for 2 hours of mixing.

To prepare the alkaline solution in RSW, the alkali was added to the seawater sample which resulted in a solution with a pH of about 9.2, which was similar to the SSW case.

3.3.2 Zeta Potential Measurements

To investigate the stability of P-NP solutions, zeta potential tests were conducted by using the apparatus Zetasizer Nano ZS by Malvern Panalytical which is presented in Figure 13. Particles having zeta potentials between -10 mV and +10 mV rapidly aggregate, whereas particles with zeta potentials less than -15 mV show acceptable stability. The concentration of nanoparticles was fixed for all performed measurements, while polymer concentration was varied by 1000 ppm, 1500 ppm, and 2500 ppm. Therefore, SiO_2 was prepared as a baseline. Each test was measured 3 times to get accurate values.

Figure 13. Zetasizer Nano ZS

3.3.3 Core Crushing

Due to the large size of the cores for direct milling, the core crushing process was divided into two steps. Initially, a Jaw Crusher machine by RETSCH which is illustrated in Figure 14, was used to break the core into millimeter-sized fragments. The RETSCH Disc Mill device was used to grind down pieces into micrometric particles afterward, which is presented in Figure 15. The final form of both Berea and Uzen cores was as powders and used for the static adsorption tests.

Figure 14. Jaw Crusher bb 250XL

Figure 15. Disc Mill DM200

3.3.4 Core Preparation

Six cores were used for core flooding tests. After being placed in an oven at 63 ºC for a day, each core sample was dried until a stable weight was achieved, indicating the complete removal of all moisture from the pore space. Dry weights and dimensions of all cores were then measured. Hereafter, depending on the type of test, the core samples were saturated with certain brine which is presented in Table 4. The saturation process was continued for one day at the pressure of 1000-1100 psi. After pulling the cores out of the device, their wet weights were measured to calculate the porosity. The apparatus used for saturation was Manual Saturator by Vinci company which is demonstrated in Figure 16.

Table 4. The plan for core saturation

Types of tests	Core rock	Saturation brine
Injectivity and dynamic adsorption	Berea	SSW
	Uzen	RSW
Oil displacement	Uzen	FW

Figure 16. Manual Saturator

3.3.5 UV Testing

The concentration of elements in a sample can be determined by using an analytical method known as UV-Vis spectrophotometry. The method measures how much light is

absorbed by a sample at particular wavelengths in the UV or visible range of the electromagnetic spectrum. This method was used to measure the concentration of samples.

A chemical sample is put in a cuvette, which is a tiny, clear container, to find out the concentration utilizing UV-Vis spectrophotometer Evolution 300 by Thermo Scientific which is presented in Figure 17. The spectrophotometer, a device that can detect the amount of light passing through the material, is then placed within the cuvette.

Accordingly, polymer concentration after static or dynamic adsorption can be determined by knowing three values: polymer absorbance at the recognized wavelength, molar absorptivity, as well as cuvette path length. This can be accomplished by utilizing a calibration curve, which is a graph of absorbance against concentration for a variety of previously determined chemical values. Finally, being informed of initial and final concentrations of polymer, both static and dynamic adsorptions can be evaluated.

Figure 17. Ultraviolet-visible spectrophotometer

3.3.6 Rheology Testing

The polymer, P-NP, and P-A samples were extracted from the core plugs after core flooding and tested using the modular compact Anton Paar rheometer (MCR 302) which is shown in Figure 18. The extracted solution was dissolved in the brine at a predetermined concentration before being used to get the samples ready.

Figure 18. Modular compact rheometer

A modular compact rheometer is used to determine a solution's viscosity. The rheometer includes a revolving spindle and a stationary cup that holds the substance under evaluation. The spindle is rotated at a predetermined speed, and the rotational resistance is obtained to assess the sample's viscosity at the temperature of 63°C, as well as the shear rate of 10 s^{-1}. The amount of dynamic adsorption onto the rock surfaces can be determined by comparing the viscosity of the polymer solution before and after core flooding.

3.3.7 Static Adsorption Tests

To investigate the adsorption of fluids on various surfaces, static adsorption studies are widely accepted. In this case, the adsorption of ASP3 on Berea sandstone and Uzen rock was analyzed throughout periods of 3, 12, 24, and 36 hours. The effects of silicon dioxide and caustic soda on polymer adsorption were also examined by applying the P-NP and P-A solutions for static adsorption experiments.

Primarily, 160 g of every solution was poured into 4 vials with 40 g each. Hereafter 10 g of the crushed core was added to each vial to achieve a liquid-to-solid ratio (L/S) of 4. The static adsorption test included measuring 34 different samples in total. The vials were placed in the roller oven to mix properly for 3 hours, 12 hours, 24 hours, and 36 hours. The device is illustrated in Figure 19 and manufactured by OFI Testing Equipment. The samples were then diluted 10 times and analyzed using a UV-Vis Spectrophotometer after two days to

enable the precipitation of the tiny particles. The reason for diluting effluents is the resolution of the apparatus, which provides more accurate results for lower solution concentrations of up to 500 ppm.

Figure 19. The OFITE roller oven

3.3.8 Injectivity and Dynamic Adsorption Tests

In general, five core flooding experiments involving injectivity and dynamic adsorption tests were carried out. To evaluate the dynamic adsorption values, nanoparticles and alkalis were used and the results were compared to the standalone polymer case. The details of the tests are provided in Table 5, where the first test was considered a trial approach.

Table 5. Specification of injectivity and dynamic adsorption tests

#	Type of the test	Type of the core rock	The sequence of injection fluids
1	Injectivity	Berea sandstone	SSW → Polymer → Postflush
	Dynamic adsorption		SSW → Polymer → SSW → Polymer → Postflush
2	Injectivity	Uzen formation	RSW → Polymer → Postflush
3	Dynamic adsorption	Uzen formation	FW → Polymer → RSW → Polymer → Postflush
4	Dynamic adsorption	Uzen formation	FW → P-NP → RSW → P-NP → Postflush
5	Dynamic adsorption	Uzen formation	FW → P-A → RSW → P-A → Postflush

All tests were conducted by the Vinci core flooding system CFS 700. The schematic illustration of the system is shown in Figure 20, where the main elements are (1-3) accumulators A, B, and C, (4) injection pumps, (5) confining pump, (6) hydrostatic core holder, (7) pressure sensors, and (8) back pressure regulator.

The conditions given to the device were the confining pressure of 1200 psi, the back pressure of 300 psi, the temperature value of 63°C, and a flow rate of 0.5 cc/min.

All dynamic adsorption tests had 2 cycles of solution injections, where each cycle consisted of certain pore volumes (PV) of the solution. Hence, the same volumes of injected fluid were collected after the production for further analysis through Rheometer and UV-Vis spectrophotometer. For instance, in the case of Berea core, overall, 10 PVs of the polymer solutions were injected, and 6 samples from each PV were gathered. In total, 252 samples were obtained from dynamic adsorption tests, and 36 samples from injectivity tests.

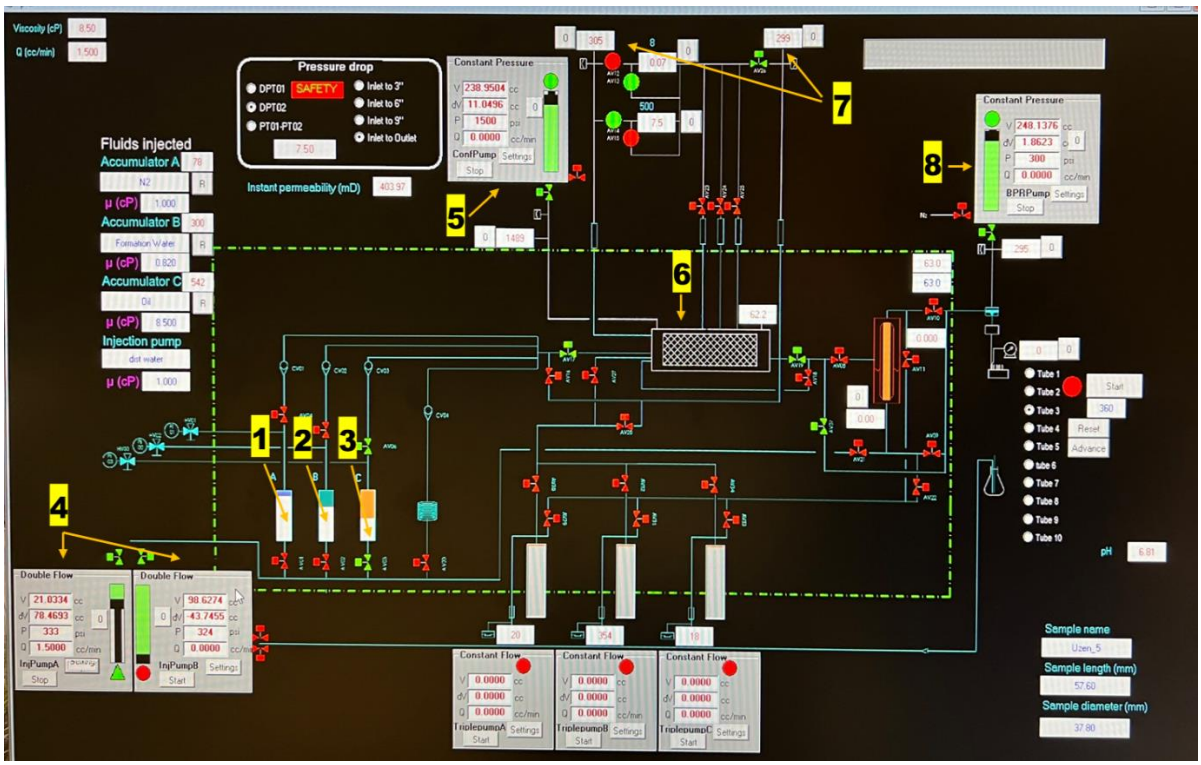

Figure 20. Computer diagram of CFS 700

Finally, analyzed data was used to calculate the value of dynamic adsorption by Equation 2.

$$q_{dynamic} = \left\{\left[\sum\left[\left(\frac{C_p}{C_{po}} \times \Delta PV\right) - \left(\frac{C_t}{C_{to}} \times \Delta PV\right)\right]\right] + IAPV\right\} \times C_{po} \times \frac{PV}{M_{rock}} \quad (2)$$

where C_p and C_{po} indicate effluent and original concentrations of the polymer; PV represents obtained pore volume of the effluent; C_t and C_{to} symbolize final and initial tracer concentrations; $IAPV$ means inaccessible pore volume; M_{rock} stands for the mass of the rock.

3.3.9 Oil Displacement Experiments

The efficiency of utilizing nanoparticles to enhance the performance of polymers for CEOR applications is measured by an oil displacement experiment that involves injecting polymer with and without nanoparticles. These experiments were carried out by use of CFS 700 at the same conditions that were applied for dynamic adsorption and injectivity investigations. Only the rate of the solution injection was altered, and it was performed in increasing sequence for each fluid injection: 0.5 cc/min, 1 cc/min, 1.5 cc/min, and 2 cc/min. The sequence of the tests is provided in Figure 21.

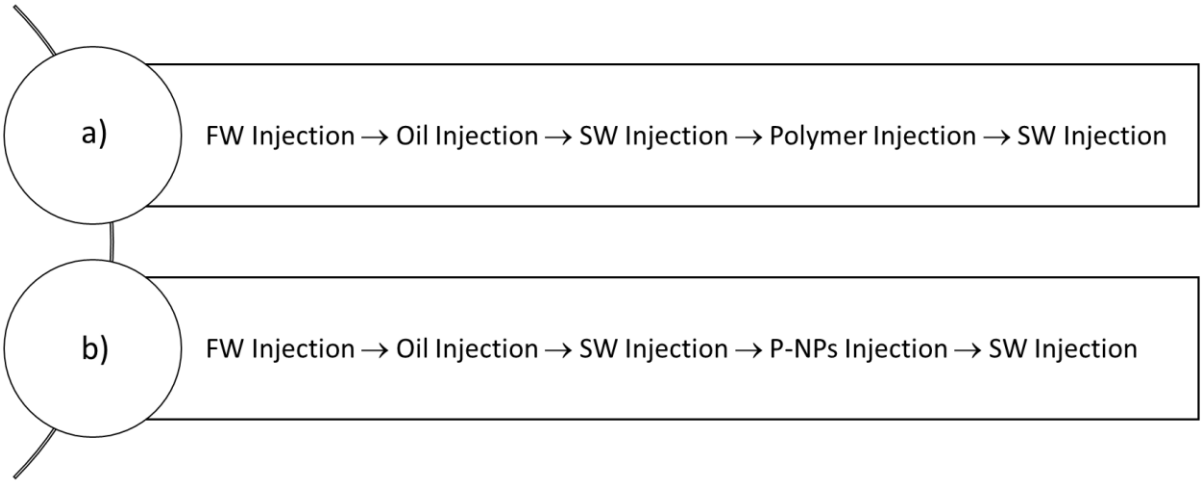

Figure 21. Design for oil displacement with polymer injection: (a) in the absence of nanoparticles, (b) in the presence of nanoparticles

The effluents were collected after the injections of seawater, solution, and postflush to define the recovered oil volume. Overall, 114 samples were collected during the oil displacement by polymer, and 98 samples were gathered during the experiment of polymer-nanoparticle flooding.

4. RESULTS AND DISCUSSION

The objective point of the conducted laboratory experiments was the evaluation of the SiO_2 efficacy in reducing ASP3 adsorption on the Uzen formation rock through obtaining static and dynamic adsorption results. Moreover, the efficiency of NaOH to decrease polymer adsorption was also investigated and described properly.

4.1 Stability Tests for Solutions

Several concentrations of the ASP3 polymer solution—1000 ppm, 1500 ppm, and 2500 ppm—were mixed with 0.1 wt. % of SiO_2 for stability experiments. Figure 22 demonstrates the visual stability of those solutions, while Table 6 presents their zeta potential values. Accordingly, zeta potential reaches a minimum of -21.7 mV at a polymer concentration of 2500 ppm. Moreover, there were no precipitations observed, implying that the mixture of nanofluid and polymer is more stable at higher polymer concentrations.

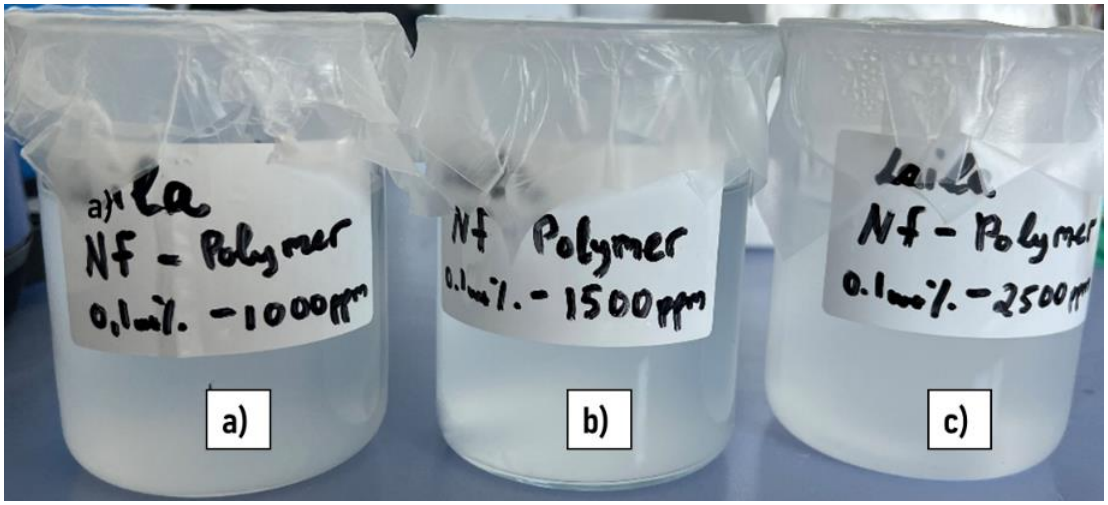

Figure 22. Variously concentrated ASP3 solutions with 0.1 wt.% SiO2: (a) 1000ppm, (b) 1500 ppm, (c) 2500 ppm

Table 6. Zeta potential test results

Test number	Solution type	Polymer concentration, ppm	Zeta potential, mV
1	Nanofluid	-	-13.7
2	Nanofluid - Polymer	1000	-11.6
3	Nanofluid - Polymer	1500	-12.1
4	Nanofluid - Polymer	2500	-21.7

Visual observation can be used to confirm the stability. Sedimentation is negligible or absent in stable solutions. Thus, different concentrations of the silica nanoparticles were evaluated. The visual observations in Figure 23 showed that the solution with a concentration of 0.3 wt. % SiO2 nanoparticles is unstable, as a large amount of precipitation is present. In contrast, the solutions with concentrations of 0.05 wt. % and 0.1 wt. % appear to be stable, as there is no sedimentation visible.

The polymer (2500ppm)-alkali (0.03%) solution also demonstrated stability, with a zeta potential of -19.6 mV.

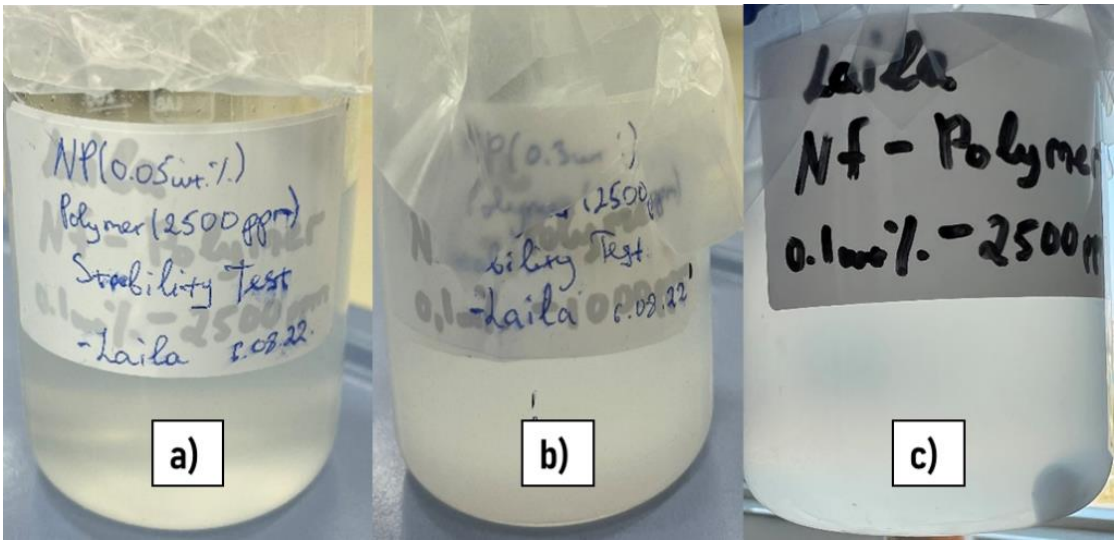

Figure 23. Varied concentrated SiO_2 solutions with 2500 ppm ASP3: (a) 0.05 wt. %, (b) 0.3 wt. %, (c) 0.1 wt. %

4.2 Calibration Curves

A graph known as a calibration curve illustrates the relationship between polymer concentration and absorbance for a polymer solution applying UV-Vis Spectrophotometer. To construct this curve, it is necessary to prepare numerous solutions with known polymer concentrations. The absorbance was then plotted as a function of the polymer concentration to create the calibration curve. For SSW-based solutions, solutions with polymer concentrations of 100 ppm and 150 ppm were prepared and their absorbance was measured, as presented in Figure 24.

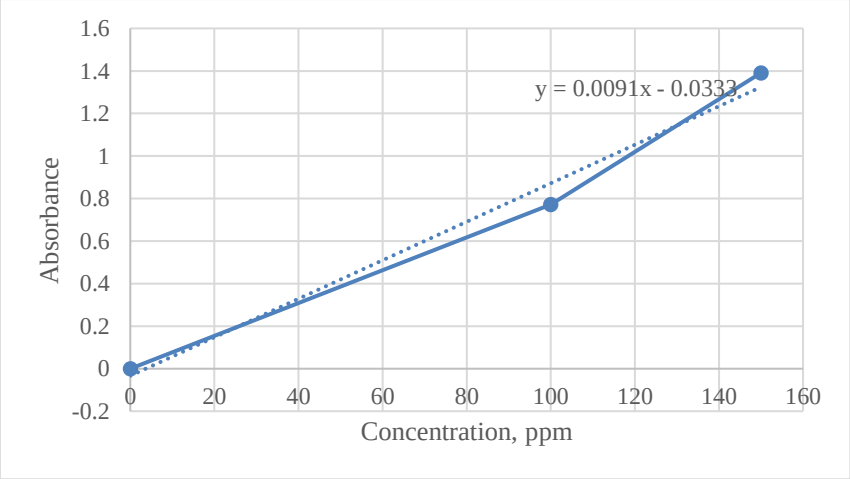

Figure 24. Calibration curve for ASP3 polymer solution in SSW

For RSW-based polymer solutions, solutions with polymer concentrations of 50 ppm, 100 ppm, 150 ppm, and 200 ppm were utilized, as shown in Figure 25. Once the calibration curve was established, it was used to estimate the unknown concentration of the polymer solution by measuring its physical property and interpolating the value on the curve. Both mentioned calibration curves were used to determine the obtained concentration of ASP3 after static adsorption tests.

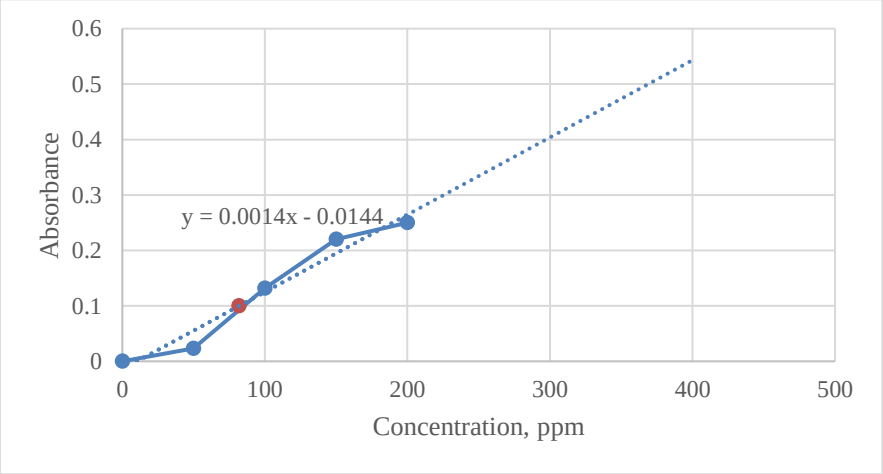

Figure 25. Calibration curve for ASP3 polymer solution based in RSW

For dynamic adsorption tests, different calibration curves were created by adding potassium iodide as a tracer into the brine, as illustrated in Figure 26 and Figure 27. In core flood experiments, a tracer is frequently added to polymer solutions to monitor the flow of the solution through the porous material. The use of a tracer makes it possible to determine and measure the volume of polymer solution that has passed the core sample. The usage of potassium iodide is due to the fact that it is a salt that dissolves in water and is easy to detect through UV-visible spectrophotometry. The amount of light that potassium iodide absorbs at

a certain wavelength is proportional to the amount of the tracer present in the solution. The breakthrough time of the polymer solution and the volume of polymer maintained within the core may both be calculated by tracking the absorbance of the tracer at the core sample's effluent. Adding a tracer to polymer solutions during core flood experiments is a crucial step in determining how well polymer flooding performs as an improved oil recovery strategy.

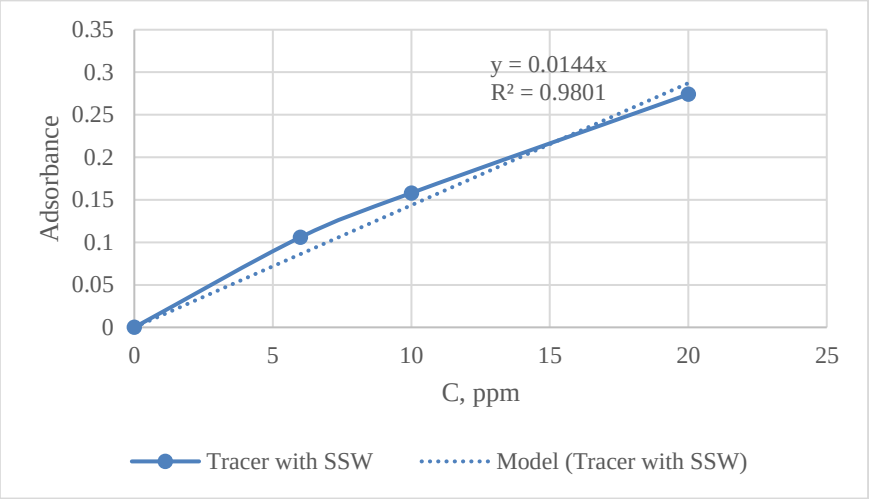

Figure 26. Calibration curve for ASP3 solution in SSW and tracer

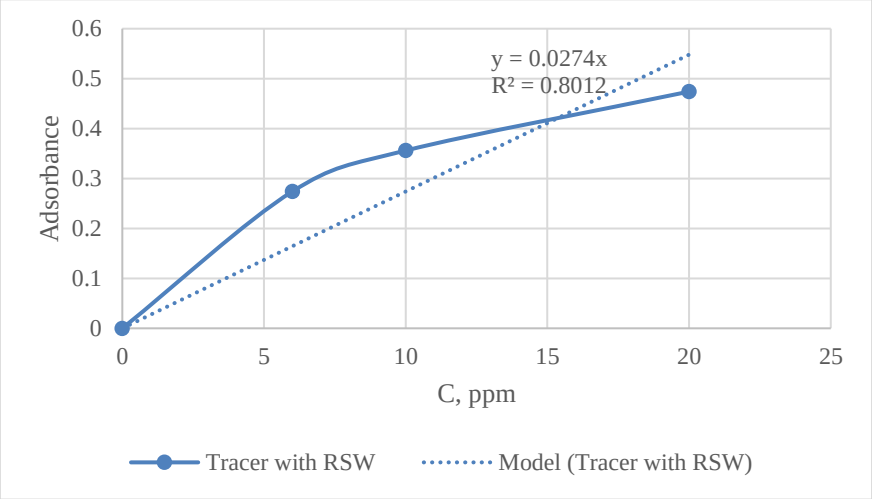

Figure 27. Calibration curve for ASP3 solution in RSW and tracer

4.3 Static Adsorption Experiments

4.3.1 Berea Sandstone Case

Table 7 displays the outcomes of static adsorption studies performed on crushed Berea Sandstone samples that were treated with various polymer solutions over time. The standalone polymer with a concentration of 2500 ppm was examined (P). The combination of

polymer with two different concentrations of silica nanoparticles (0.05wt% and 0.1wt%), and in combination with an alkaline solution was also analyzed. The values for adsorption listed in Table 6 are expressed in µg/g, which represents the quantity of polymer adsorbed per gram of solid material. Also, Figure 28 represents the results at different times.

Table 7. Static adsorption tests on Berea sandstone

	Adsorption, µg/g			
t, hrs	**P**	**P-NP (0.05)**	**P-NP (0.1)**	**P-A**
3	940.09	948.88	947.56	943.16
12	952.84	954.59	956.35	954.15
24	973.05	962.07	957.23	962.07
36	976.13	967.78	963.82	970.86

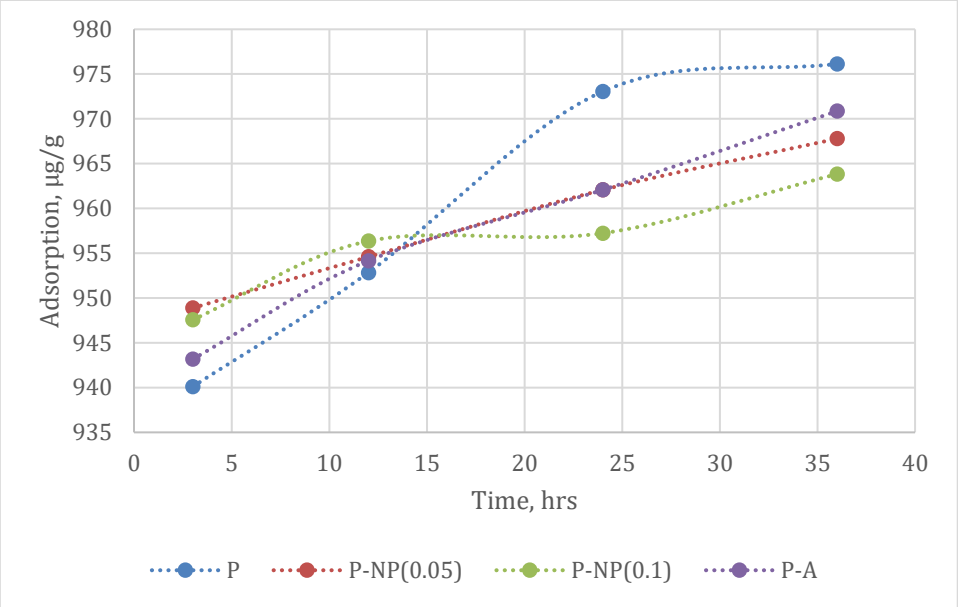

Figure 28. Polymer adsorption by time on Berea rock

The adsorption values after three hours ranged from 940 µg/g for P to 948 µg/g for P-NP (0.05wt%), which was quite similar for all the treatments. This shows that the addition of sodium hydroxide solution or silica nanoparticles did not have a substantial impact on the polymer's initial adsorption. This can be explained by the reason that both alkali and NPs required some residence time to interact with polymer and rock surfaces.

The adsorption values increased for all treatments at the 12-hour mark, with P-NP (0.1wt%) displaying the highest value at 956 µg/g. P and P-A both had high adsorption

values, 953 µg/g, and 954 µg/g, respectively. This shows that despite the difference in the treatment, the polymer's adsorption increased with time.

The adsorption values kept rising at the 24-hour mark, with P showing the highest values (973 µg/g). P-NP (0.05wt%) and P-A adsorption values were the same by 962 µg/g, indicating a lower value than for the polymer instance. Applying P-NP (0.1wt%) resulted in the lowest amount of adsorption achieving 957 µg/g. This shows that the application of silica nanoparticles is effective in lowering the polymer's adsorption over a longer period.

The adsorption values for all treatments reached their highest levels at 36 hours, ranging from 963 µg/g for P-NP (0.1wt%) to 976 µg/g for P. This shows that the polymer's adsorption increased over time but comparatively less with the application of SiO_2.

Overall, the findings indicate that the treatment had an impact on the HPAM-based polymer's ability to adhere to crushed Berea Sandstone, with the addition of an alkaline solution (P-A) improving this process. Nevertheless, over extended periods of time, the alkaline solution's impact lessened and the adsorption values for P and P-A converged. At the same time, nanoparticles have a longer-lasting and more persistent effect on adsorption decrease.

4.3.2 Uzen Formation Case

Table 8 presents the findings of static adsorption tests conducted on crushed samples of Uzen field formation rock. Regarding Figure 29, it can be seen that for all treatments, the quantity of adsorption tended to rise over time. This may be explained by the fact that more polymer molecules adhere to the surface of the rock over time, increasing the quantity of adsorption.

Table 8. Static adsorption tests on Uzen rock

	Adsorption, µg/g			
t, hrs	**P**	**P-NP (0.05)**	**P-NP (0.1)**	**P-A**
3	756	750.29	624.57	467.43
12	784.57	790.29	616	564.57
24	827.43	821.71	736	770.29
36	884.57	896	850.29	793.14

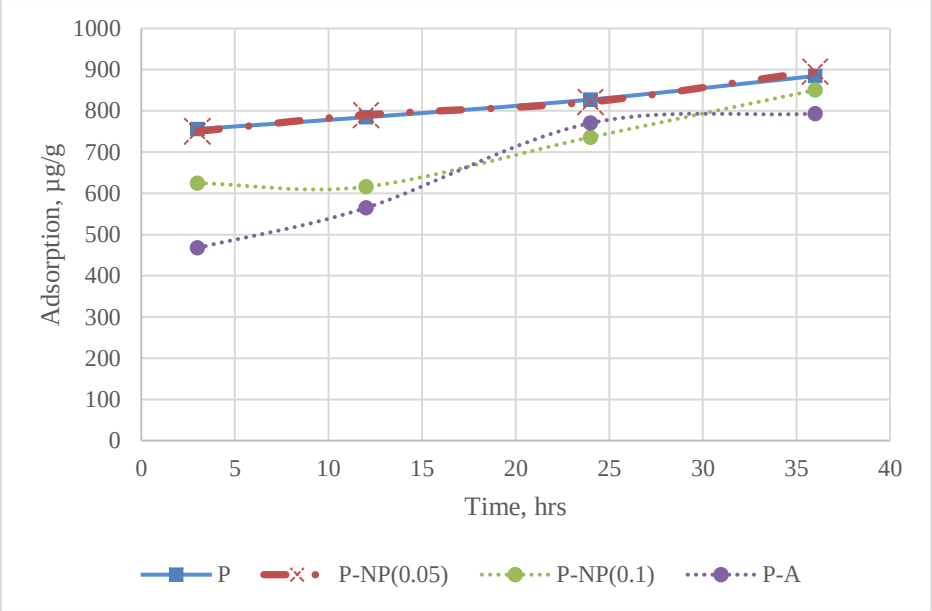

Figure 29. Polymer adsorption by time on Uzen crushed rock

The polymer solution containing 0.1wt% silica nanoparticles had the least quantity of adsorption (850.29 g/g). This is caused by the fact that compared to the standalone polymer, the nanoparticles have a larger surface area and a more active surface. Due to the nanoparticles' active surface, fewer sites are accessible for polymer adsorption as a result of the nanoparticles' ability to compete with the polymer for adsorption sites on the rock surface.

When a polymer is combined with an alkaline solution, the adsorption of the polymer showed decreased values. This is because the alkaline solution makes the rock's surface more negatively charged, repelling the negatively charged polymer molecules and reducing the amount of polymer adsorption.

Overall, the study showed that the capacity of the ASP3 polymer to adsorb onto the Uzen rock during longer contact times can be diminished by the addition of silica nanoparticles or an alkaline solution. It is important to note that these findings are particular to the experimental setup performed and that more research may be required to support these conclusions.

4.4 Polymer Performance in Porous Media

The outcomes of all types of core flood tests show how applied polymers behave in a porous medium. In particular, injectivity tests are carried out to assess the reservoir's capacity for fluid injection and the fluid's efficacy in raising the mobility ratio. Moreover, the test measures the polymer solution's capacity to go through a porous medium without generating significant pressure drops or harm to the formation.

According to Table 9, the test utilizing the Berea core obtained an RF of 75.89 using Formula 3, the value indicates that the injected polymer flows about 76 times slower than the injected water. In the injectivity experiment outcomes involving the Uzen core which is shown in Table 10, the RF was 112.67, which is greater than the RF of the prior test with Berea sandstone. A high resistance factor found during a polymer injectivity test can show that the injected polymer is efficiently blocking high permeable channels and displacing fluids in the reservoir, which can contribute to enhancing sweep efficiency. When the injected fluid displaces the reservoir fluids continuously and uniformly, without fingering, this is known as piston-like displacement. By ensuring that the injected fluid is spread evenly throughout the reservoir, a high resistance factor can contribute to enhancing piston-like displacement by maintaining the pressure gradient and preventing an early breakthrough.

$$RF = \frac{\Delta p_{chemical\ flood}}{\Delta p_{preflush}} \quad (3)$$

$$RRF = \frac{\Delta p_{brine}}{\Delta p_{preflush}} \quad (4)$$

Table 9. Results of injectivity test on Berea rock

	DP, psi	DP, atm	q, cc/min	q, cc/s	Calculated k_{abs}, mD	RF
SSW Injection	0.55	0.04	0.5	0.01	131.53	
Polymer Injection	41.74	2.84	0.5	0.01	44.49	75.89
Postflush	8.23	0.56	0.5	0.01	8.79	

Table 10. Results of injectivity test on Uzen rock

	DP, psi	DP, atm	q, cc/min	q, cc/s	Calculated k_{abs}, mD	RF
RSW Injection	1.5	0.10	0.5	0.01	30.58	
Polymer Injection	169	11.50	0.5	0.01	7.57	112.67
Postflush	78.8	5.36	0.5	0.01	0.58	

Concerning dynamic adsorption tests, it was determined how much polymer is adsorbed and trapped in the porous media during the polymer flooding.

The results of the trial test utilizing the Berea core are presented in Table 11, where the value of RRF after post-flushing of one cycle of ASP 3 injection was equal to 14.96. Calculation of the RRF is shown in Formula 4. As the polymer adheres to the sample surface, it might obstruct the pore throats and diminish the rock's permeability which leads to a

pressure drop in the system. This occurs as a result of the fluid experiencing more resistance and requiring more force to get through the rock due to its difficulty passing through it. So, an RRF of about 15 means that not all injected polymer was displaced from the core by postflush brine, this implies that it was adsorbed, trapped, or retained on the rock. Completing the post-flushing of the second cycle of the polymer, RRF displayed 46.53, indicating that almost half of the initially injected polymer volume was still present in the core.

Table 11. Dynamic adsorption test in Berea sandstone core

	DP, psi	DP, atm	q, cc/min	q, cc/s	Calculated k_{abs}, mD	RF	RRF
SSW Preflush	0.55	0.04	0.5	0.01	131.53		
Polymer Cycle-1	41.74	2.84	0.5	0.01	44.49	75.89	
SSW Injection	8.23	0.56	0.5	0.01	8.79		14.96
Polymer Cycle-2	112.43	7.65	0.5	0.01	16.52	204.42	
SSW Postflush	25.59	1.74	0.5	0.01	2.83		46.53

The data provided in Tables 12 to 14 clearly show that the RF values have consistently increased in all three cases: polymer flooding, polymer flooding with alkali, and polymer flooding with nanoparticles during the flooding to the Uzen field cores. This trend suggests that the application of chemical flooding techniques has increased fluid flow resistance. Nevertheless, the presence of alkali can affect the charge on the polymer, which can alter its rheology, decreases its viscosity, and reduce its effectiveness in reducing fluid flow resistance. The addition of nanoparticles, on the contrary, makes the fluid viscous and improves RF. The viscosity of the P-NPs solution achieved 38.0 cP, while only the ASP3 solution was 22.0 cP. As it is seen that viscosity was nearly doubled, therefore the value of RF was also almost increased 2 times.

Table 12. Dynamic adsorption test in Uzen field core for the standalone polymer flooding

	DP, psi	DP, atm	q, cc/min	q, cc/s	Calculated k_{abs}, mD	RF	RRF
RSW Preflush	0.47	0.03	0.5	0.01	105.15		
Polymer Cycle-1	114.11	7.76	0.5	0.01	12.15	241.47	
RSW Injection	28.49	1.94	0.5	0.01	1.74		60.28
Polymer Cycle-2	100.24	6.82	0.5	0.01	13.83	212.11	
RSW Postflush	31.99	2.18	0.5	0.01	1.55		67.70

Table 13. Dynamic adsorption test in Uzen field core in presence of alkali

	DP, psi	DP, atm	q, cc/min	q, cc/s	Calculated k_{abs}, mD	RF	RRF
RSW Preflush	0.19	0.01	0.5	0.01	251.99		
P-A Cycle-1	36.91	2.51	0.5	0.01	43.52	194.24	
RSW Injection	5.80	0.39	0.5	0.01	8.25		30.53
P-A Cycle-2	29.80	2.03	0.5	0.01	53.90	156.84	
RSW Postflush	8.93	0.61	0.5	0.01	5.36		46.99

Table 14. Dynamic adsorption test in Uzen field core in presence of 0.5 wt.% nanoparticles

	DP, psi	DP, atm	q, cc/min	q, cc/s	Calculated k_{abs}, mD	RF	RRF
RSW Preflush	0.63	0.04	0.5	0.01	75.48		
P-NP Cycle-1	293.94	20.00	0.5	0.01	7.74	469.22	
RSW Injection	33.30	2.27	0.5	0.01	1.42		53.15
P-NP Cycle-2	286.42	19.49	0.5	0.01	7.94	457.21	
RSW Postflush	93.78	6.38	0.5	0.01	0.50		149.71

The tables also provide the RRF values that demonstrate the residual polymer in the porous medium. Comparing the outcomes demonstrated that SiO_2 application has little or no effect on the remaining polymer and does not increase trapping, which is favorable. The RRF for the combination of P-NPs was 53.15, which was even lower than the RRF for pure polymer flooding (60.28).

Moreover, high mechanical degradation occurred in all three experiments (Figures 30-32) with Uzen rock due to the high polymer concentration of 2500 ppm and large viscosity of 22.0 cP. Factors that caused this high degradation level are the high shear rate and polymer retention (adsorption, trapping, and entrapment). Shear forces that the polymer solution may experience as it passes through the rock may cause it to break into smaller pieces.

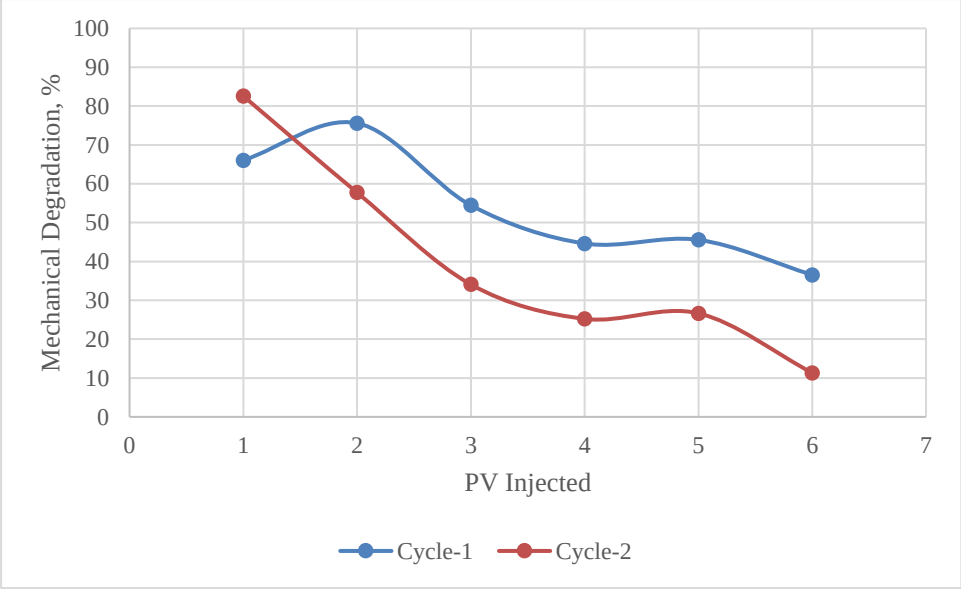

Figure 30. Mechanical degradation of polymer solution in Uzen core

In addition, the findings suggest that the HPAM polymer solution's mechanical deterioration during the core flooding tests is influenced by the addition of alkaline and nanoparticles. Adding sodium hydroxide to the polymer solution can also lead to degradation since it creates hydroxide ions that can damage the polymer chains. As a result, the solution's viscosity and efficiency may drop. In the case of the P-NPs solution, the addition of nanoparticles increased the viscosity of the solution, which also caused a higher level of mechanical degradation.

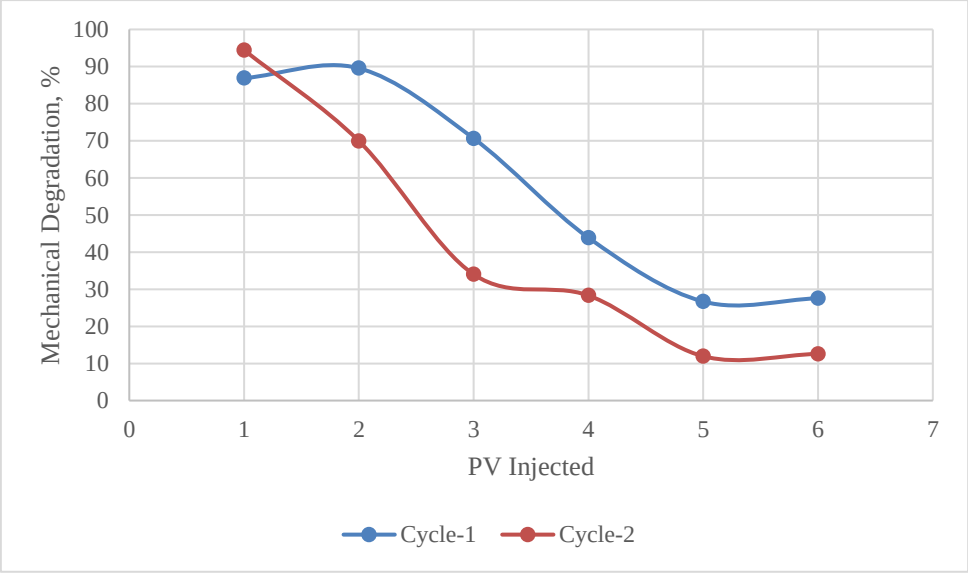

Figure 31. Mechanical degradation of polymer-alkali solution in Uzen core

When comparing all the examples, the degree of mechanical degradation after the injection of the second cycle of solutions was much lower than during the first cycle. The

chemical molecules, particularly polymer chains, may have partially covered the rock surface after the first cycle due to their capacity to adsorb onto mineral surfaces or become trapped in the pore spaces of the rock matrix. This reason is also explains the trend of mechanical degradation decrease in all cases. As a result, this could reduce the surface area available for further rock-fluid interactions during subsequent injection cycles. In addition, the retention of polymer chains might cause a thin polymer layer to form on the rock's surface, acting as a barrier to additional adsorption and chemical deterioration. This could improve the general efficacy of following injection cycles.

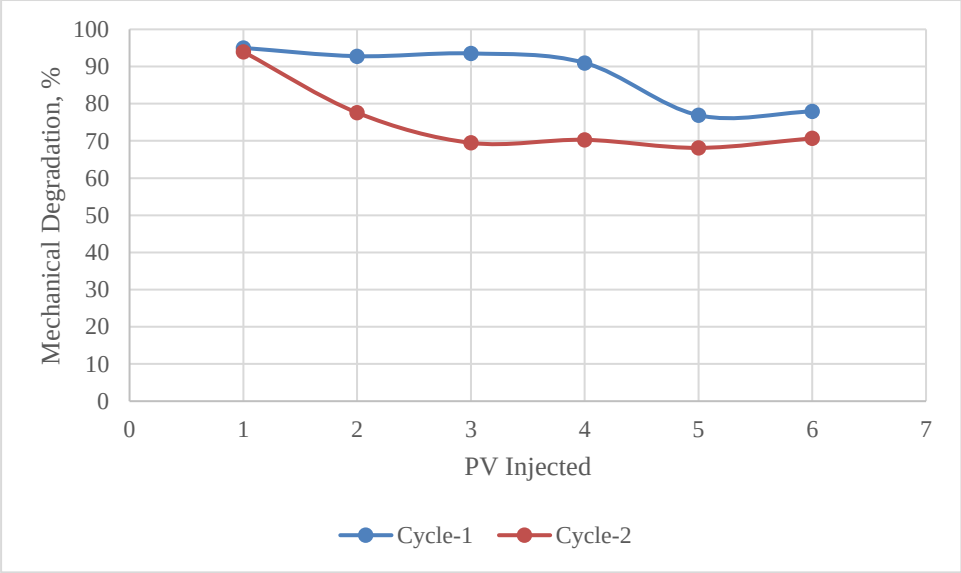

Figure 32. Mechanical degradation of polymer-nanoparticles solution in Uzen core

4.5 Dynamic Adsorption Tests

The process of a substance adhering to a solid surface while flowing constantly is referred to as dynamic adsorption. The amount of polymer adsorbed onto a solid matrix was assessed over time in dynamic adsorption studies, which included flowing a solution containing the polymer over the core at a regulated rate of 0.5 cc/min. Moreover, chemicals like NaOH and SiO_2 were combined with the polymer and used as an injection fluid to lessen the adsorption of the polymer during the flooding.

The trial dynamic adsorption test was carried out on Berea sandstone, and Figure 33 displays the pressure drop values during the injection of polymer solution into the pores. A viscosity profile was initially constructed utilizing the viscosity-concentration profile from the Rheometer. It was a primary step in estimating the value of dynamic adsorption by

Formula 1. As shown in Figure 34, the viscosity profile was used to obtain concentration values from the presented two equations. For observed viscosities, less than 16 cP, the equation on the left-bottom side of the figure was employed, and for values more than 16 cP, another equation was.

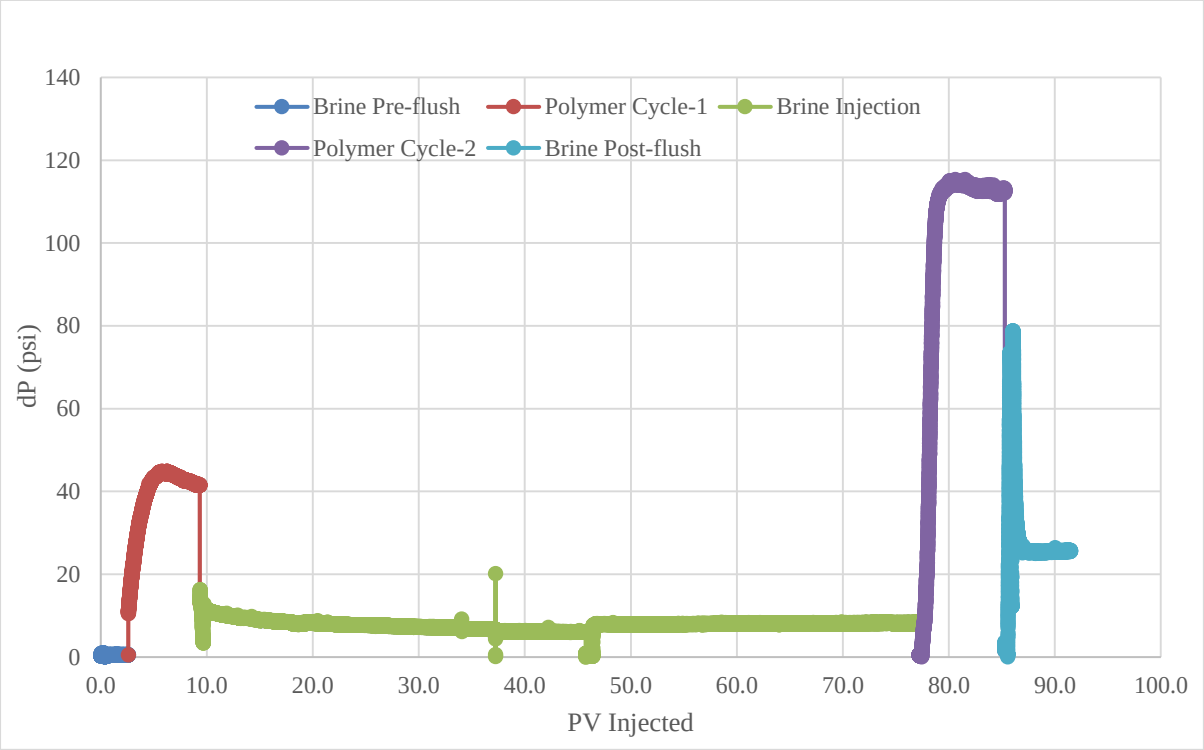

Figure 33. Pressure drop profile of dynamic adsorption test in Berea

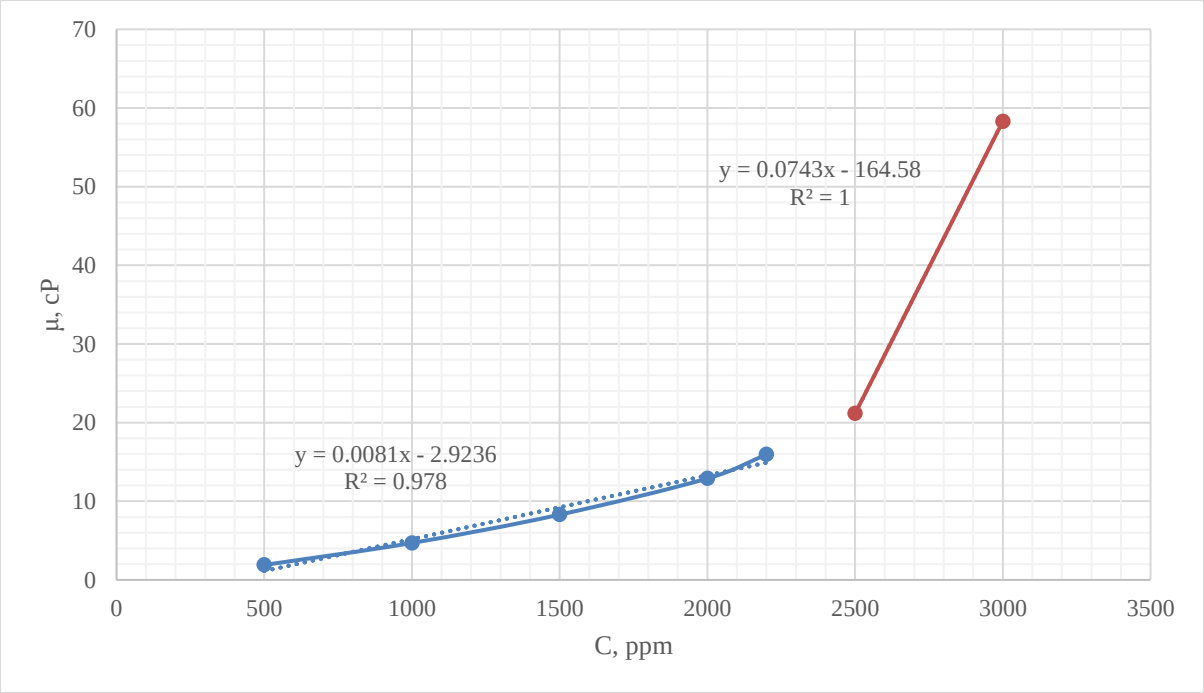

Figure 34. Viscosity profile of ASP 3 at different concentrations

After that, based on the evaluated concentrations, incremental and cumulative viscosities of the effluents from both polymer cycles were calculated and used to get the IAPV value. As displayed in Figure 35, two chosen points for each cycle indicate after how many pore volumes, 50% of the polymer was produced. Following that, Equation 5 was applied to calculate IAPV. For the case, the value was 22.27%.

$$IAPV = \frac{Injected\ PV(cycle\ 1) - Injected\ PV(cycle\ 2)}{Injected\ PV(cycle\ 1)} \times 100\% \quad (5)$$

Following that the measurement of the tracer effluents was taken using UV-Vis equipment, and the tracer concentrations were computed based on the calibration curve and absorbance values. Hereafter, the last unknown value which is the mass of rock was estimated through Equation 6, and was equal to 181.34 g. The data on rock characteristics were taken from Table 1.

$$M_{rock} = (BV - PV) \times \rho_{rock} \quad (6)$$

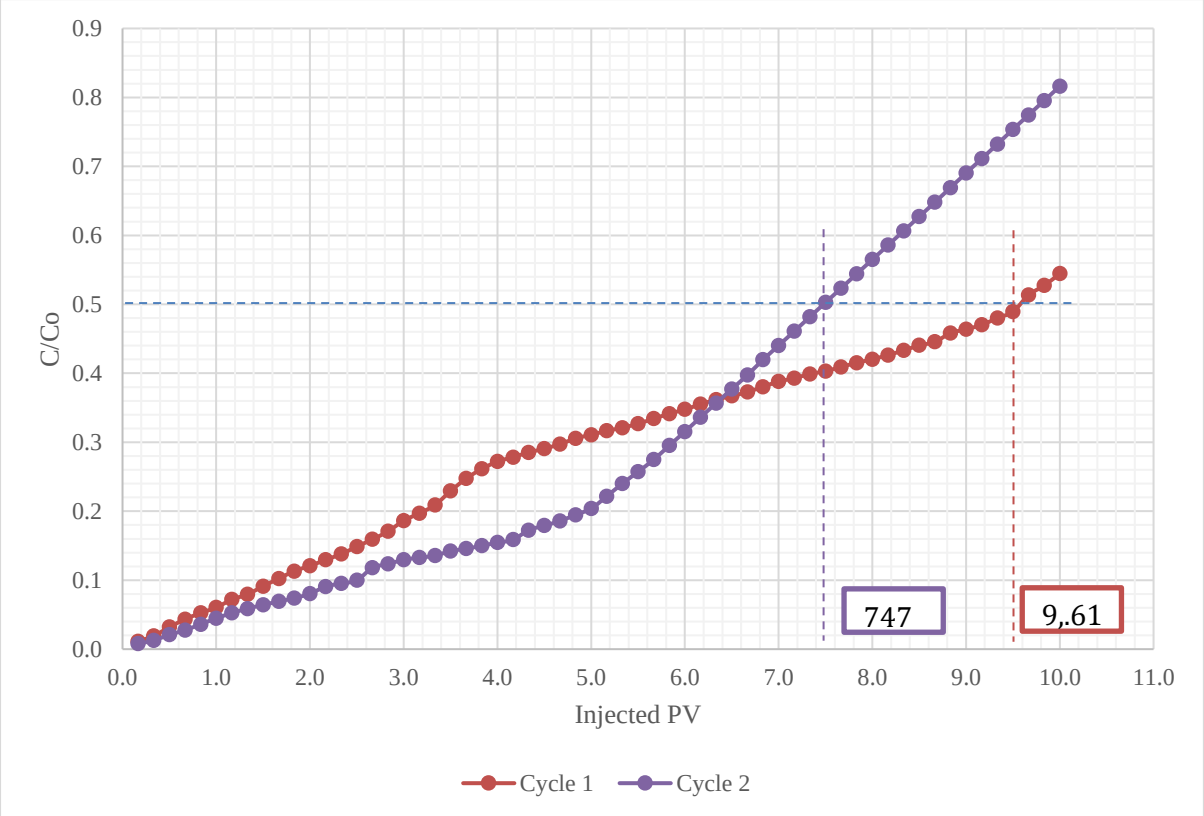

Figure 35. Polymer production through Berea core at different injection cycles

Finally, the evaluated value of the dynamic adsorption for the test using Berea sandstone was calculated through Formula 2 as 600.385 μg/$g_{(rock)}$. The same steps were repeated to estimate dynamic adsorption values from experiments with Uzen cores. Table 15 provides the results of the IAPV and dynamic adsorption.

Table 15. The dynamic adsorption and IAPV values of tests using Uzen cores

Injected fluid	Dynamic adsorption, μg/$g_{(rock)}$	IAPV, %
Polymer	766.43	7.87
Polymer-Alkali	805.90	13.19
Polymer-Nanoparticles	632.40	44.83

It is clear from the data in Table 15 that adding alkali to the polymer solution causes both an increase in dynamic adsorption—from 766.426 μg/g of rock to 805.9 μg/g of rock—and an increase in IAPV—from 7.87% to 13.19%. This shows that alkali did not reduce polymer adsorption as intended and instead caused more fluid to be adsorbed onto the rock surface. That can be explained by the findings of static adsorption studies, in which polymer adsorption increased instantly after 12 hours of contact with the Uzen rock. As the polymer charge was not negative enough, the repulsive force between the rock and the polymer was weak.

On the other hand, the dynamic adsorption of the polymer solution decreases when nanoparticles are added, changing from 766.426 μg/g (rock) to 632.398 μg/g (rock). Despite this, IAPV significantly increased from 7.87% to 44.83%. That can be clarified by the fact that the pressure drop was significantly increased since the solution's viscosity was twice as high. Nevertheless, as the permeability values were the same, it is assumed that nanoparticles have not blocked pores more than in the case of standalone polymer flooding.

4.6 Oil Displacement Tests

To increase the oil recovery from the Uzen field, polymer flooding was used for the oil displacement test. Our results showed that silica nanoparticle is more effective to enhance the performance of polymer flooding. Hence, the effect of adding this nanoparticle to the polymer flooding on the oil recovery and oil fluid flow in the Uzen field media was also investigated. Two cases were analyzed without and in presence of silica nanoparticles, to evaluate the impact of reducing polymer adsorption on sweeping more oil.

The Uzen core saturation showed 20% of saturation with FW after the injection of oil in the first experiment with polymer case. Original oil in place (OOIP) was calculated by the

information in Table 1 and using Equation 5. The estimated value of OOIP was 12.16 cc. Pressure drops outcomes of preflush and oil injection are presented in Figure 36.

$$OOIP = AL\varphi\left(1 - \frac{S_{wi}}{100}\right) \quad (5)$$

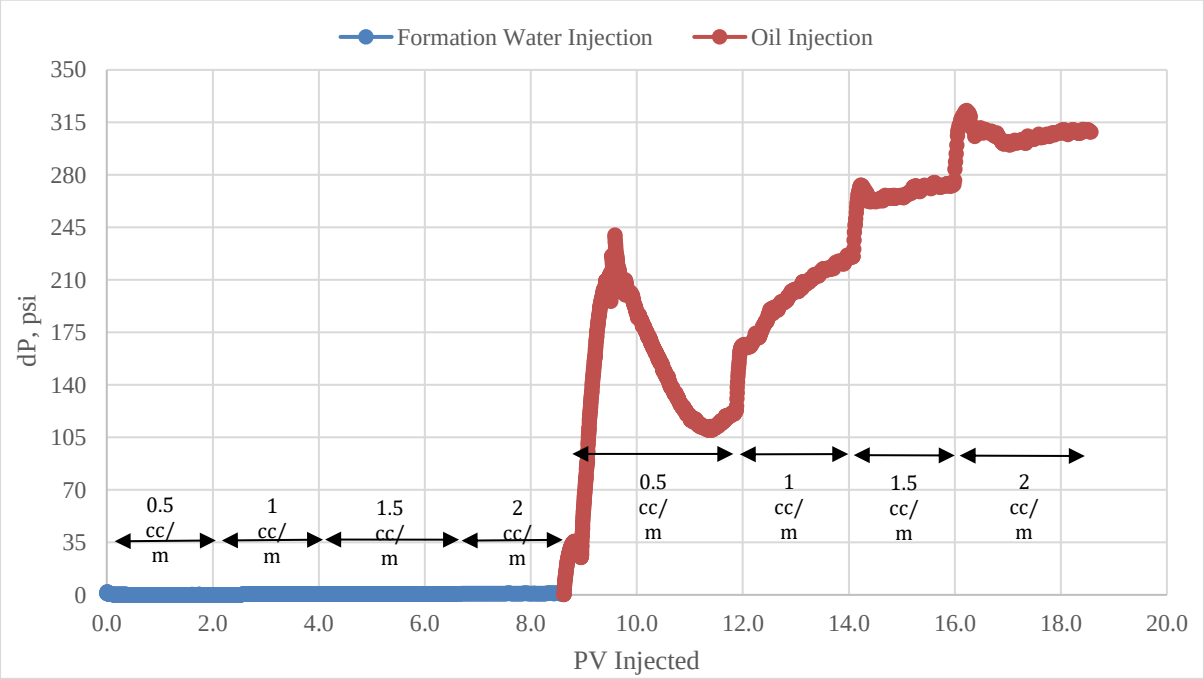

Figure 36. Pressure change profile for FW and oil injections in Case 1

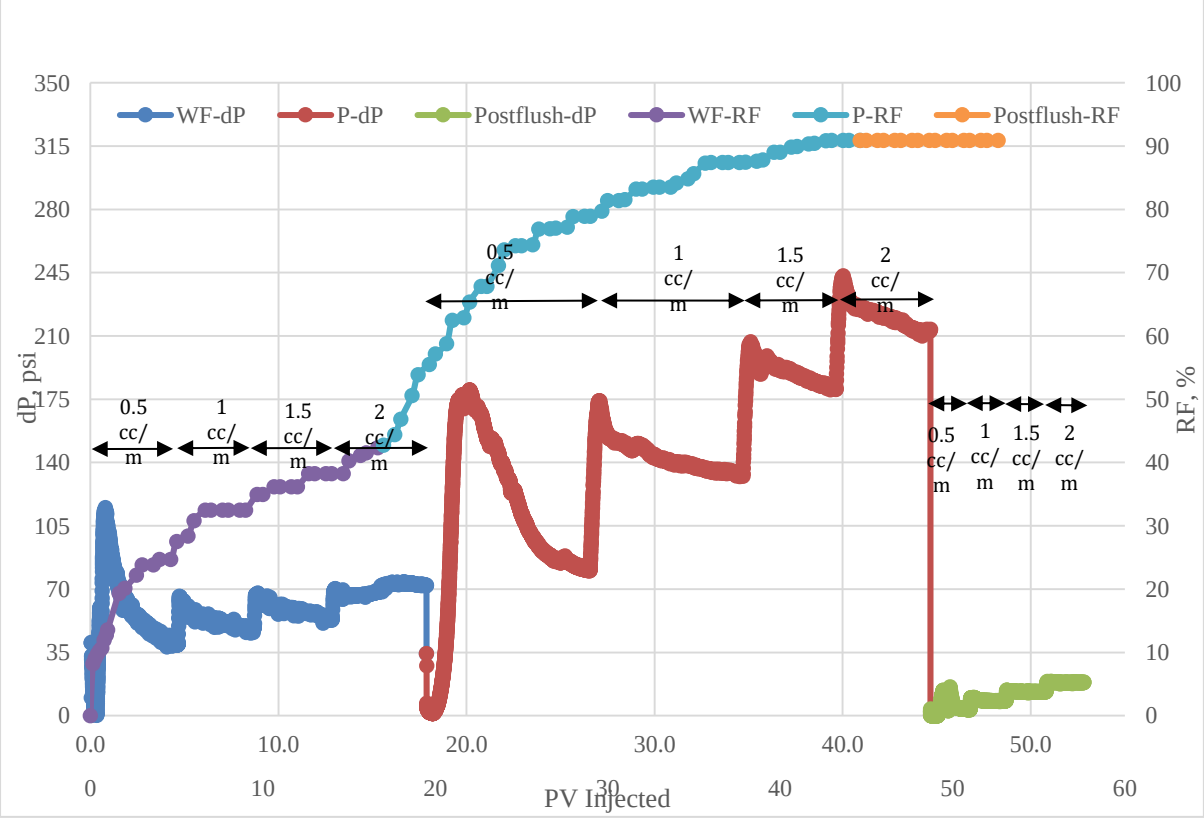

Figure 37. Pressure change and recovery factor profiles for RSW, polymer, and postflush injections in Case 1

After saturating the core with oil, 17 PV of RSW was injected, resulting in 42.8% of the oil recovery factor. Next, 27 PV of 2500 ppm polymer solution was applied, achieving a recovery factor of 90.9%. So, the detailed results of RF, pressure drop by injected PV are shown in Figure 37.

In the second oil displacement case with injection of polymer-nanoparticles solution, the Uzen core was saturated with FW by 25% after oil flooding, and OOIP showed 11.69%. Related pressure drop values during the first two injection processes are presented in Figure 38. Also, according to Figure 39, about 49.51% of oil was produced by injecting 22 PV of RSW, while 18 PV of injected ASP3-SiO_2 displaced obtained 94.58% of total recovery. It is important to point out that, in both cases, the chemical injection and post-flush were continued until there was no longer any oil produced by them.

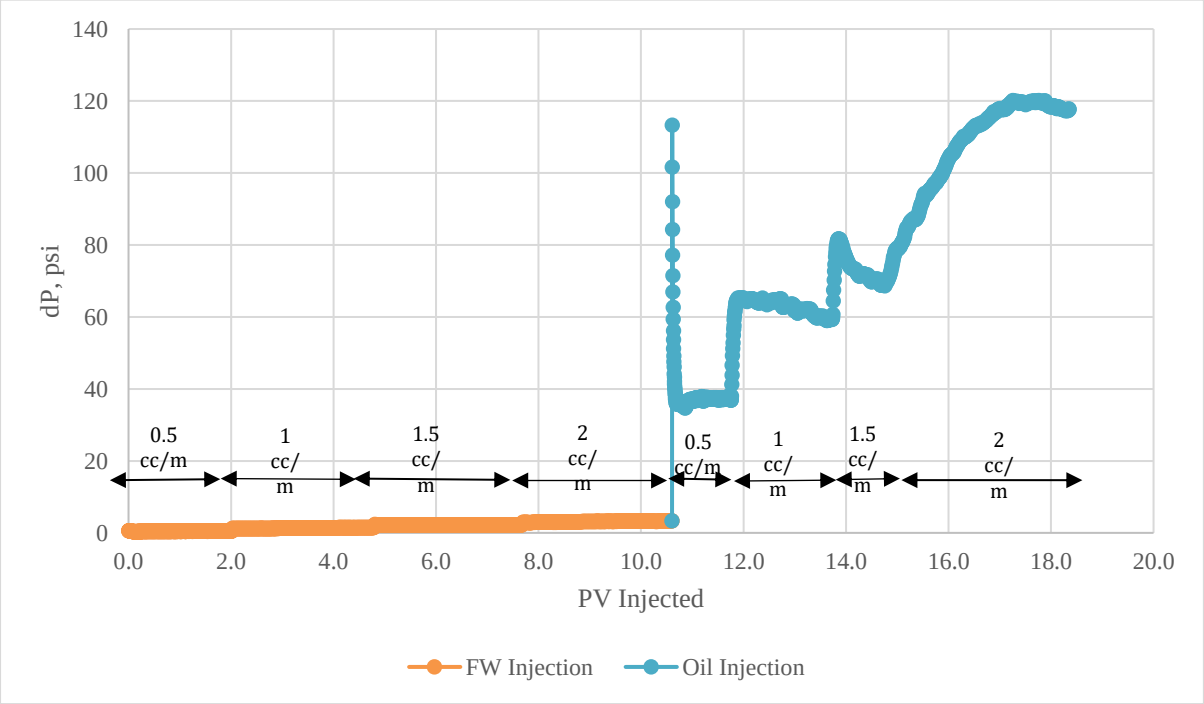

Figure 38. Pressure change profile for FW and oil injections in Case 2

In accordance with results of recovery factors presented in Table 16, the value of incremental recovery factor in terms of remaining oil in core (ROIC) after P-NPs injection was higher for more than 5% compared to solely polymer flooding. Several considerations may be used to explain the improved outcomes in the second scenario where silica nanoparticles were added to the polymer solution. Firstly, adding nanoparticles into the polymer solution can assist in decreasing the polymer's adsorption onto the rock surface, increasing the mobility of the injected fluid and enhancing oil displacement effectiveness.

Due to the decrease in polymer adsorption, there may be more polymer available to interact with the oil and enhance recovery. The second way that nanoparticles themselves can contribute to improved oil recovery is by lowering the interfacial tension and maximizing contact between the injected fluid and the oil. Finally, adding nanoparticles to the polymer solution can also lead to enhancing the fluid's rheological characteristics, enlarging viscosity which can increase its capacity to sweep the reservoir and remove more oil. This can result in a larger incremental recovery factor.

Table 16. Recovery factor results of oil displacement tests

#	Flooding	Recovery Factor	Incremental RF	Inc. RF
		(%OOIP)		(%ROIC)
1	RSW	42.8	-	-
	Polymer	90.9	48.1	**84.12**
2	RSW	49.5	-	-
	P-NPs	94.6	45.07	**89.26**

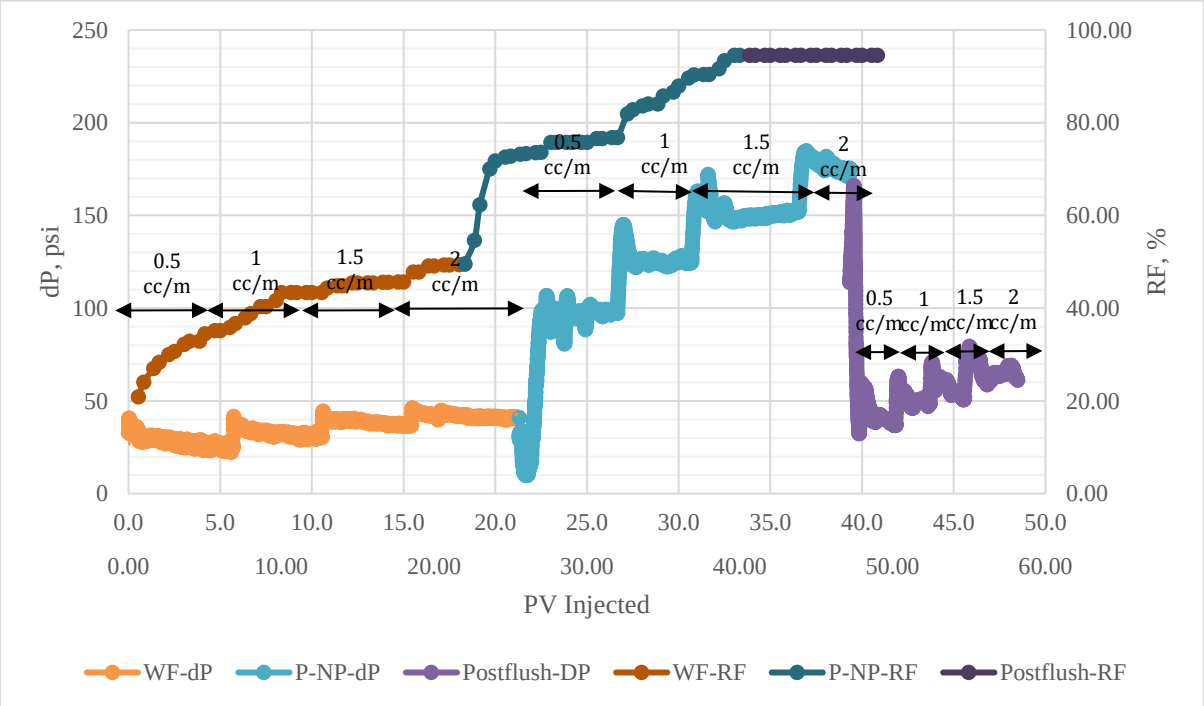

Figure 39. Pressure change and recovery factor profiles for RSW, polymer, and postflush injections in Case 2

5. CONCLUSIONS AND RECOMMENDATIONS

This work was aimed to reduce ASP3 polymer adsorption on the formation rock of the Uzen field with the use of chemicals, such as silica nanoparticles, and sodium hydroxide functioning as alkaline. Favorable mixtures of the chemicals were obtained through visual and zeta potential screenings resulting P (2500 ppm) – A (0.03%), P (2500 ppm) – NP (0.1 wt. %), and P (2500 ppm) – NP (0.05 wt. %). Multiple varying experiments were conducted, consequently establishing following conclusions:

- The outcomes of the static adsorption tests have shown that the combination of caustic soda and ASP3 was ineffective in extended durations of time, particularly after reaching 12 hours of interaction with rock. Observed phenomenon confirmed the unsuccessful dynamic adsorption research, where adding alkali showed a reverse impact on the polymer adsorption, increasing it by nearly 40 $\mu g/g_{(rock)}$.
- Among P-NPs solutions, the application of a mixture with 0.1 wt% SiO_2 demonstrated significantly decreased ASP3 adsorption on the Uzen rock during static adsorption tests.
- It was observed that the rise in RRF was noticed at the same ratio as the increase in viscosity of the solution after the addition of SiO_2.
- The lowest value of polymer dynamic adsorption was found as 632.398 $\mu g/g_{(rock)}$ that accounted for the case of P-NP injection. It was less for 134.028 $\mu g/g_{(rock)}$ in comparison to just polymer injection instance.
- According to the results of the oil displacement tests, the P-NP application had a larger incremental recovery of 89.26%, which was higher by 5.14% than the scenario with simply polymer flooding. That can be explained by the research demonstrating that the addition of SiO2 increased the polymer's viscosity and considerably reduced its adsorption.

On the basis of the study's findings, several recommendations for further study are provided. As the successful performance of nanoparticles application in diminishing ASP3 was determined, other types of CEOR as surfactant-polymer and alkali-surfactant-polymer methods can be tested for efficacy as well. Additionally, different alkalis and nanoparticles can be investigated to observe the impact on ASP3 polymer adsorption.

6. REFERENCES

Abbas, S., Sanders, A. W., & Donovan, J. C. (2013, July). Applicability of hydroxyethylcellulose polymers for chemical EOR. In *SPE Enhanced Oil Recovery Conference*. OnePetro. https://doi.org/10.2118/165311-MS

Abidin, A. Z., Puspasari, T., & Nugroho, W. A. (2012). Polymers for enhanced oil recovery technology. *Procedia Chemistry*, *4*, 11-16. https://doi.org/10.1016/j.proche.2012.06.002

Al-Hajri, S., Mahmood, S. M., Abdulelah, H., & Akbari, S. (2018). An overview on polymer retention in porous media. *Energies*, *11*(10), 2751. https://doi.org/10.3390/en11102751

Al-Hajri, S., Negash, B. M., Rahman, M. M., Haroun, M., & Al-Shami, T. M. (2021). Effect of Silica Nanoparticles on Polymer Adsorption Reduction on Marcellus Shale. *ACS omega*, *6*(44), 29537-29546. https://pubs.acs.org/doi/full/10.1021/acsomega.1c03653

Alfazazi, U., AlAmeri, W., & Hashmet, M. R. (2018, November). Screening of new HPaM base polymers for applications in high temperature and high salinity carbonate reservoirs. In *Abu Dhabi International Petroleum Exhibition & Conference*. OnePetro.

https://doi.org/10.2118/192805-MS

Ali, L., & Barrufet, M. A. (1994). Profile modification due to polymer adsorption in reservoir rocks. *Energy & fuels*, *8*(6), 1217-1222. https://pubs.acs.org/doi/pdf/10.1021/ef00048a008

Alsofi, A. M., Wang, J., Leng, Z., Abbad, M., & Kaidar, Z. F. (2017, April). Assessment of polymer interactions with carbonate rocks and implications for EOR applications. In *SPE Kingdom of Saudi Arabia Annual Technical Symposium and Exhibition*. OnePetro.

https://doi.org/10.2118/188086-MS

Ambaliya, M., & Bera, A. (2023). A Perspective Review on the Current Status and Development of Polymer Flooding in Enhanced Oil Recovery Using Polymeric Nanofluids. *Industrial & Engineering Chemistry Research*, *62*(6), 2444-2459.

https://pubs.acs.org/doi/pdf/10.1021/acs.iecr.2c04582

American Petroleum Institute. (1990). *Recommended practices for evaluation of polymers used in enhanced oil recovery operations* (1st ed. June 1 1990). American Petroleum Institute. Retrieved April 3 2023 from http://books.google.com/books?id=6d5XAAAAYAAJ.

Bealessio, B. A., Alonso, N. A. B., Mendes, N. J., Sande, A. V., & Hascakir, B. (2021). A review of enhanced oil recovery (EOR) methods applied in Kazakhstan. *Petroleum*, *7*(1), 1-9.

https://doi.org/10.1016/j.petlm.2020.03.003

Bedrikovetsky, P. (1997, August). Improved waterflooding in reservoirs of highly paraffinic oils. In *Latin American and Caribbean Petroleum Engineering Conference*. OnePetro. https://doi.org/10.2118/39083-MS

Belhaj, A. F., Elraies, K. A., Mahmood, S. M., Zulkifli, N. N., Akbari, S., & Hussien, O. S. (2020). The effect of surfactant concentration, salinity, temperature, and pH on surfactant adsorption for chemical enhanced oil recovery: a review. *Journal of Petroleum Exploration and Production Technology*, *10*, 125-137. https://doi.org/10.1007/s13202-019-0685-y

Bodratti, A. M., Sarkar, B., Song, D., Tsianou, M., & Alexandridis, P. (2015). Competitive adsorption between PEO-containing block copolymers and homopolymers at silica. *Journal of Dispersion Science and Technology*, *36*(1), 1-9. https://doi.org/10.1080/01932691.2014.880847

Chengara, A., Nikolov, A. D., Wasan, D. T., Trokhymchuk, A., & Henderson, D. (2004). Spreading of nanofluids driven by the structural disjoining pressure gradient. *Journal of colloid and interface science*, *280*(1), 192-201. https://doi.org/10.1016/j.jcis.2004.07.005

Cheraghian, G. (2017). Evaluation of clay and fumed silica nanoparticles on adsorption of surfactant polymer during enhanced oil recovery. *Journal of the Japan Petroleum Institute*, *60*(2), 85-94. https://doi.org/10.1627/jpi.60.85

Cheraghian, G., Khalili Nezhad, S. S., Kamari, M., Hemmati, M., Masihi, M., & Bazgir, S. (2014). Adsorption polymer on reservoir rock and role of the nanoparticles, clay and SiO2. *International Nano Letters*, *4*, 1-8. https://doi.org/10.1007/s40089-014-0114-7

Choi, B., Jeong, M. S., & Lee, K. S. (2014). Temperature-dependent viscosity model of HPAM polymer through high-temperature reservoirs. *Polymer degradation and stability*, *110*, 225-231. https://doi.org/10.1016/j.polymdegradstab.2014.09.006

CIA. (1982). *Uzen Oilfield: A Case Study of Soviet Mismanagement.* https://www.cia.gov/readingroom/docs/CIA-RDP83B00851R000400050002-6.pdf

Corredor Rojas, L. M. (2019). The Impact of Surface Modified Nanoparticles on the Performance of Polymer Solutions for Heavy Oil Recovery. http://dx.doi.org/10.11575/PRISM/36812

Dang, T. Q. C., Chen, Z., Nguyen, T. B. N., & Bae, W. (2014). Investigation of isotherm polymer adsorption in porous media. *Petroleum science and technology*, *32*(13), 1626-1640.

https://doi.org/10.1080/10916466.2010.547910

Dang, C. T., Chen, Z., Nguyen, N. T., Bae, W., & Phung, T. H. (2011, September). Development of isotherm polymer/surfactant adsorption models in chemical flooding. In *SPE Asia Pacific oil and gas conference and exhibition*. OnePetro. https://doi.org/10.2118/147872-MS

Dash, J. G. (2012). *Films on solid surfaces: the physics and chemistry of physical adsorption*. Elsevier. https://www.sciencedirect.com/book/9780122033506/films-on-solid-surfaces

Ekanem, E. M., Rücker, M., Yesufu-Rufai, S., Spurin, C., Ooi, N., Georgiadis, A., ... & Luckham, P. F. (2021). Novel adsorption mechanisms identified for polymer retention in carbonate rocks. *JCIS Open*, *4*, 100026. https://doi.org/10.1016/j.jciso.2021.100026

Firozjaii, A. M., & Saghafi, H. R. (2020). Review on chemical enhanced oil recovery using polymer flooding: Fundamentals, experimental and numerical simulation. *Petroleum*, *6*(2), 115-122. https://doi.org/10.1016/j.petlm.2019.09.003

Gbadamosi, A. O., Junin, R., Manan, M. A., Yekeen, N., & Augustine, A. (2019). Hybrid suspension of polymer and nanoparticles for enhanced oil recovery. *Polymer Bulletin*, *76*, 6193-6230. https://link.springer.com/article/10.1007/s00289-019-02713-2

Ghalamizade Elyaderani, S. M., & Jafari, A. (2020). Investigation of interactions between silica nanoparticle, alkaline, and polymer in micromodel flooding for enhanced oil recovery. *Energy Sources, Part A: Recovery, Utilization, and Environmental Effects*, 1-18. https://doi.org/10.1080/15567036.2020.1811428

Hall, L. M., Jayaraman, A., & Schweizer, K. S. (2010). Molecular theories of polymer nanocomposites. *Current Opinion in Solid State and Materials Science*, *14*(2), 38-48. https://doi.org/10.1016/j.cossms.2009.08.004

Hincapie, R. E., Borovina, A., Clemens, T., Hoffmann, E., Tahir, M., Nurmi, L., ... & Janczak, A. (2022). Optimizing Polymer Costs and Efficiency in Alkali–Polymer Oilfield Applications. *Polymers*, *14*(24), 5508. https://doi.org/10.3390/polym14245508

Janiga, D., Czarnota, R., Stopa, J., Wojnarowski, P., & Kosowski, P. (2017). Performance of nature inspired optimization algorithms for polymer enhanced oil recovery process. *Journal of Petroleum Science and Engineering*, *154*, 354-366. https://doi.org/10.1016/j.petrol.2017.04.010

Jung, J. C., Zhang, K., Chon, B. H., & Choi, H. J. (2013). Rheology and polymer flooding characteristics of partially hydrolyzed polyacrylamide for enhanced heavy oil recovery. *Journal of Applied Polymer Science*, *127*(6), 4833-4839. http://dx.doi.org/10.1002/app.38070

Imanbayev, B., Kushekov, R., Sagyndikov, M., & Shyrakbayev, D. (2022, November). Feasibility Study of a Polymer Flood for the Uzen Brownfield Conditions. In *SPE Annual Caspian Technical Conference*. OnePetro. https://doi.org/10.2118/212091-MS

Kakati, A., Bera, A., & Al-Yaseri, A. (2022). A Review on Advanced Nanoparticles-Induced Polymer Flooding for Enhanced Oil Recovery. *Chemical Engineering Science*, 117994.

https://doi.org/10.1016/j.ces.2022.117994

Kamal, M. S., Sultan, A. S., Al-Mubaiyedh, U. A., & Hussein, I. A. (2015). Review on polymer flooding: rheology, adsorption, stability, and field applications of various polymer systems. *Polymer Reviews*, *55*(3), 491-530. https://doi.org/10.1080/15583724.2014.982821

Kazempour, M., Sundstrom, E., & Alvarado, V. (2012). Effect of alkalinity on oil recovery during polymer floods in sandstone. *SPE Reservoir Evaluation & Engineering*, *15*(02), 195-209. https://doi.org/10.2118/141331-PA

Kazmunaygas. (2007). *Uzen oilfield discovery and development history.* http://www.kmgep.kz/data/filedat/Pressreleases/Presentation_UMG_20Sept.pdf

Kazmunaygas. (2017). *Oil and gas sector.* http://www.kmgep.kz/eng/about_kazakhstan/oil_and_gas_sector/

Kotoulas, K. T., Campbell, J., Skirtach, A. G., Volodkin, D., & Vikulina, A. (2022). Surface Modification with Particles Coated or Made of Polymer Multilayers. *Pharmaceutics*, *14*(11), 2483. https://doi.org/10.3390/pharmaceutics14112483

Krumrine, P. H., & Falcone, J. S. (1983, June). Surfactant, polymer, and alkali interactions in chemical flooding processes. In *SPE Oilfield and Geothermal Chemistry Symposium*. OnePetro. https://doi.org/10.2118/11778-MS

Kurniadi, H. M., Fathaddin, M. T., & Riswati, S. S. (2022, November). Effect of Sand Grain on Adsorption of Xanthan Gum and Polyacrylamide. In *IOP Conference Series: Earth and Environmental Science* (Vol. 1104, No. 1, p. 012035). IOP Publishing.

https://iopscience.iop.org/article/10.1088/1755-1315/1104/1/012035/pdf

Lew, J. H., Matar, O. K., Müller, E. A., Maung, M. T. M., & Luckham, P. F. (2022). Adsorption of hydrolysed polyacrylamide onto calcium carbonate. *Polymers*, *14*(3), 405.

https://doi.org/10.3390/polym14030405

Li, Y., Guo, J., Wang, S., Yang, R., & Lu, Q. (2019, March). Reducing hydroxypropyl guar gum adsorption on rock by silica nanoparticles for tight reservoir damage remediation. In *International petroleum technology conference*. OnePetro. https://doi.org/10.2523/IPTC-19561-MS

Liu, J., Wei, Y., Li, P., Zhao, Y., & Zou, R. (2017). Selective H2S/CO2 separation by metal–organic frameworks based on chemical-physical adsorption. *The Journal of Physical Chemistry C*, *121*(24), 13249-13255. https://pubs.acs.org/doi/pdf/10.1021/acs.jpcc.7b04465

Ma, X., & Pawlik, M. (2005). Effect of alkali metal cations on adsorption of guar gum onto quartz. *Journal of Colloid and Interface Science*, *289*(1), 48-55. https://doi.org/10.1016/j.jcis.2005.03.035

Mahran, S., Attia, A., & Saha, B. (2018, May). A review on polymer flooding in enhanced oil recovery under harsh conditions. In *11th International Sustainable Energy & Environmental Protection Conference*. https://openresearch.lsbu.ac.uk/item/86qz2

Mishra, S., Bera, A., & Mandal, A. (2014). Effect of polymer adsorption on permeability reduction in enhanced oil recovery. *Journal of Petroleum Engineering*, *2014*. http://dx.doi.org/10.1155/2014/395857

Mohammed, I., Afagwu, C. C., Adjei, S., Kadafur, I. B., Jamal, M. S., & Awotunde, A. A. (2020). A review on polymer, gas, surfactant and nanoparticle adsorption modeling in porous media. *Oil & Gas Science and Technology–Revue d'IFP Energies nouvelles*, *75*, 77.

https://doi.org/10.2516/ogst/2020063

Mohd, T. T., Taib, N. M., Adzmi, A. F., Ab Lah, N. N., Sauki, A., & Jaafar, M. Z. (2018). Evaluation of polymer properties for potential selection in enhanced oil recovery. *Chemical Engineering Transactions*, *65*, 343-348. https://doi.org/10.3303/CET1865058

Muhammed, N. S., Haq, M. B., Al-Shehri, D., Rahaman, M. M., Keshavarz, A., & Hossain, S. Z. (2020). Comparative study of green and synthetic polymers for enhanced oil recovery. *Polymers*, *12*(10), 2429. https://doi.org/10.3390/polym12102429

Mullaev, B. T., Abitova, A. Zh., Turkpenbayeva, B. Zh., & Saenko, O. B. (2016). *Uzen Field: Problems and Solutions* (Vol.1), Strelbitsky's multimedia publishing house, 75-392.

https://books.google.kz/books?id=RSZKDwAAQBAJ&printsec=frontcover#v=onepage&q&f=false

Navaie, F., Esmaeilnezhad, E., & Choi, H. J. (2022). Effect of Rheological Properties of Polymer Solution on Polymer Flooding Characteristics. *Polymers*, *14*(24), 5555.

https://doi.org/10.3390/polym14245555

Nurmi, L., Hincapie, R. E., Clemens, T., Hanski, S., Borovina, A., Födisch, H., & Janczak, A. (2022). Improving Alkali Polymer Flooding Economics by Capitalizing on Polymer Solution Property Evolution at High pH. *SPE Reservoir Evaluation & Engineering*, 1-16.

https://doi.org/10.2118/210043-PA

O'Shea, J. P., Qiao, G. G., & Franks, G. V. (2010). Solid–liquid separations with a temperature-responsive polymeric flocculant: effect of temperature and molecular weight on polymer adsorption and deposition. *Journal of colloid and interface science*, *348*(1), 9-23.

https://doi.org/10.1016/j.jcis.2010.04.063

Park, H., Han, J., & Sung, W. (2015). Effect of polymer concentration on the polymer adsorption-induced permeability reduction in low permeability reservoirs. *Energy*, *84*, 666-671. https://doi.org/10.1016/j.energy.2015.03.028

Pu, W., Shen, C., Wei, B., Yang, Y., & Li, Y. (2018). A comprehensive review of polysaccharide biopolymers for enhanced oil recovery (EOR) from flask to field. *Journal of Industrial and Engineering Chemistry*, *61*, 1-11. https://doi.org/10.1016/j.jiec.2017.12.034

Quadri, S. M., Jiran, L., Shoaib, M., Hashmet, M. R., AlSumaiti, A. M., & Alhassan, S. M. (2015, November). Application of biopolymer to improve oil recovery in high temperature high salinity carbonate reservoirs. In *Abu Dhabi international petroleum exhibition and conference*. OnePetro. https://doi.org/10.2118/177915-MS

Quinten, T., De Beer, T., Remon, J. P., & Vervaet, C. (2011). Overview of injection molding as a manufacturing technique for pharmaceutical application. *Injection molding: process, design and application. New York: Nova*, 1-42.

https://www.researchgate.net/publication/287590984_Overview_of_injection_molding_as_a_manufacturing_technique_for_pharmaceutical_applications

Rellegadla, S., Prajapat, G., & Agrawal, A. (2017). Polymers for enhanced oil recovery: fundamentals and selection criteria. *Applied microbiology and biotechnology*, *101*, 4387-4402. https://doi.org/10.1007/s00253-017-8307-4

Rudi, N. N., Muhamad, M. S., Te Chuan, L., Alipal, J., Omar, S., Hamidon, N., ... & Harun, H. (2020). Evolution of adsorption process for manganese removal in water via agricultural waste adsorbents. *Heliyon*, *6*(9), e05049. https://doi.org/10.1016/j.heliyon.2020.e05049

Ruiz-Cañas, M. C., Quintero-Perez, H. I., Castro-Garcia, R. H., & Romero-Bohorquez, A. R. (2020). Use of nanoparticles to improve thermochemical resistance of synthetic polymer to enhanced oil recovery applications: A review. *CT&F-Ciencia, Tecnología y Futuro*, *10*(2), 85-97. https://doi.org/10.29047/01225383.259

Sagir, M., Mushtaq, M., Tahir, M. S., Tahir, M. B., & Shaik, A. R. (2020). *Surfactants for enhanced oil recovery applications* (pp. 65-87). Cham: Springer. https://link.springer.com/book/10.1007/978-3-030-18785-9

Satken, B. (2021). Adsorption/Retention of Polymer Solution in Porous Media. *Doctoral dissertation, Bordeaux*.

https://theses.hal.science/tel-03267834/file/SATKEN_BAUYRZHAN_2021.pdf

Scott, A. J., Romero-Zerón, L., & Penlidis, A. (2020). Evaluation of polymeric materials for chemical enhanced oil recovery. *Processes*, *8*(3), 361. https://doi.org/10.3390/pr8030361

Sheng, J. J. (2017). Critical review of alkaline-polymer flooding. *Journal of Petroleum Exploration and Production Technology*, *7*, 147-153. https://doi.org/10.1007/s13202-016-0239-5

Sheng, J. J. (Ed.). (2013). *Enhanced oil recovery field case studies*. Gulf Professional Publishing. http://dx.doi.org/10.1016/C2010-0-67974-0

Sparke, S. J., Kislyakov, P. Y., & Amirtayev, M. A. (2005, June). Significant production enhancement in uzen field, kazakhstan through surface and subsurface optimization. In *SPE Europec/EAGE Annual Conference*. OnePetro. https://doi.org/10.2118/94360-MS

Sun, X., Zhang, Y., Chen, G., & Gai, Z. (2017). Application of nanoparticles in enhanced oil recovery: a critical review of recent progress. *Energies*, *10*(3), 345. https://doi.org/10.3390/en10030345

Sveistrup, M., van Mastrigt, F., Norrman, J., Picchioni, F., & Paso, K. (2016). Viability of biopolymers for enhanced oil recovery. *Journal of Dispersion Science and Technology*, *37*(8), 1160-1169. https://doi.org/10.1080/01932691.2015.1088450

Thomas, A. (2016). Polymer flooding. *Chemical Enhanced Oil Recovery (cEOR)-a Practical Overview*, 55-99. https://www.intechopen.com/chapters/51645

Udoh, T. H. (2021). Improved insight on the application of nanoparticles in enhanced oil recovery process. *Scientific African*, *13*, e00873. https://doi.org/10.1016/j.sciaf.2021.e00873

Vidali, G., Ihm, G., Kim, H. Y., & Cole, M. W. (1991). Potentials of physical adsorption. *Surface Science Reports*, *12*(4), 135-181. https://doi.org/10.1016/0167-5729(91)90012-M

Vossoughi, S., & Putz, S. (1994). Application of Newly Discovered Biopolymer in Enhanced Oil Recovery. *Scientia Iranica*, *1*(3).

http://scientiairanica.sharif.edu/article_3027_a85bd0348aff9118c953f2e3a625e867.pdf

Wang, S., Li, G., Li, Y., Guo, J., Zhou, S., Yong, S., ... & Bai, B. (2017). Adsorption of new hydrophobic polyacrylamide on the calcite surface. *Journal of Applied Polymer Science*, *134*(38), 45314. https://doi.org/10.1002/app.45314

Wasan, D., Nikolov, A., & Kondiparty, K. (2011). The wetting and spreading of nanofluids on solids: Role of the structural disjoining pressure. *Current Opinion in Colloid & Interface Science*, *16*(4), 344-349. https://doi.org/10.1016/j.cocis.2011.02.001

Webb, P. A. (2003). Introduction to chemical adsorption analytical techniques and their applications to catalysis. *Micromeritics Instrument Corp. Technical Publications*, 1-12.

https://www.micromeritics.com/Repository/Files/intro_to_chemical_adsorption.pdf

Wiśniewska, M. (2011). A review of temperature influence on adsorption mechanism and conformation of water soluble polymers on the solid surface. *Journal of dispersion science and technology*, *32*(11), 1605-1623. https://doi.org/10.1080/01932691.2010.528332

Wiśniewska, M., Chibowski, S., & Urban, T. (2015). Modification of the alumina surface properties by adsorbed anionic polyacrylamide—impact of polymer hydrolysis. *Journal of Industrial and Engineering Chemistry*, *21*, 925-931. https://doi.org/10.1016/j.jiec.2014.04.034

Xie, L., Wang, J., Huang, J., Cui, X., Wang, X., Liu, Q., & Zeng, H. (2018). Anisotropic polymer adsorption on molybdenite basal and edge surfaces and interaction mechanism with air bubbles. *Frontiers in chemistry*, *6*, 361. https://doi.org/10.3389/fchem.2018.00361

Yerniyazov D., Yesmukhambet M., Kenes R., Bukayev A., Shakeel M., Pourafshary P., & Musharova D. (2023). Polymer Screening for Efficient Water Cut Reduction in a Sandstone Oilfield in Kazakhstan. *Polymers, 15(8),* 1969. https://doi.org/10.3390/polym15081969

Zerpa, L. Reservoir engineering. Colorado School of Mines, pp.9-26

Zhang, D., Du, X., Song, X., Wang, H., Li, X., Jiang, Y., & Wang, M. (2018). Application of the marangoni effect in nanoemulsion on improving waterflooding technology for heavy-oil reservoirs. *SPE Journal*, *23*(03), 831-840. https://doi.org/10.2118/187953-PA

Zhang, X., Nguyen, H., Daly, M., Nguyen, S. T., & Espinosa, H. D. (2019). Nanoscale toughening of ultrathin graphene oxide-polymer composites: mechanochemical insights into hydrogen-bonding/van der Waals interactions, polymer chain alignment, and steric parameters. *Nanoscale*, *11*(25), 12305-12316. https://doi.org/10.1039/C9NR01453E

Zhong, H., Yang, T., Yin, H., Lu, J., Zhang, K., & Fu, C. (2020). Role of alkali type in chemical loss and ASP-flooding enhanced oil recovery in sandstone formations. *SPE Reservoir Evaluation & Engineering*, *23*(02), 431-445. https://doi.org/10.2118/191545-PA

Zhong, H., Zhang, W., Fu, J., Lu, J., & Yin, H. (2017). The performance of polymer flooding in heterogeneous type II reservoirs—An experimental and field investigation. *Energies*, *10*(4), 454. https://doi.org/10.3390/en10040454

Zhu, S., Ye, Z., Liu, Z., Chen, Z., Li, J., & Xiang, Z. (2021). Adsorption characteristics of polymer solutions on media surfaces and their main influencing factors. *Polymers*, *13*(11), 1774. https://doi.org/10.3390/polym13111774

7. APPENDICES

Table 17. Polymer types used in CEOR: pros and cons

Polymer Type	Molecular Weight	Advantages	Drawbacks	References
Polyacrylamide	0.2-30 million g/mol	-Good salinity resistance	-High adsorption -Poor shear stability	(Kamal et al., 2015; Chen, 2016)
Hydrolyzed polyacrylamide	Over 10 million g/mol	-Good stability to temperatures up to 160°C -Low cost -High solubility in water	-Poor chemical stability -Poor shear stability	(Choi et al., 2014)
Xanthan Gum	2-20 million g/mol	-Less sensitive to salinity -Good shear stability	-High cost -Biodegradation -Low elasticity	(Al-Hajri et el., 2018; Kamal et al., 2015)
Hydrophobically modified associating	1-2 million g/mol	-High solubility in water -High apparent viscosity	-Dependence on L/S ratio -Poor salinity resistance	(Kamal et al., 2015)
Cellulose	5-8 million g/mol	-Environmentally friendly -Good injectivity -Good stability resistance	-Poor temperature stability	(Abbas et al., 2013)